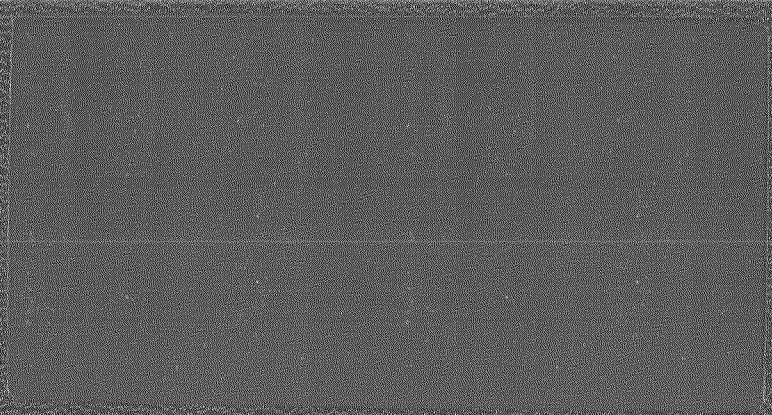

OSAKA UNIVERSITY
GRADUATE SCHOOL OF ENGINEERING SCIENCE
DEPARTMENT OF MATERIAL PHYSICS
TOYONAKA OSAKA

Microscopic theory of initial oxidation on Si(100) surfaces

Yoshiyuki Miyamoto

Fundamental Research Laboratories, NEC Corporation,
34 Miyukigaoka, Tsukuba 305, Japan

December 20, 1990

Abstract

A theoretical approach to the subject of oxidation on Si(100) surface has been presented here. We have performed the *ab–initio* total–energy band–structure and force calculations within a framework of the local density approximation for oxygen adsorbed Si(100) surfaces. The adsorbed oxygen atoms and surface Si atoms have been fully relaxed according to the calculated forces. We have found (1)dissociation of an O_2 molecule at any site on the Si(100) surface, (2)three (meta)stable sites of the adsorbed O atom on the surface, and (3)penetration of oxygen molecule through the oxygen covered surface. A peculiar distortion of Si atoms and a volume expansion of the substrate upon the oxidation have also been demonstrated. This results give us a fundamental knowledge of oxidation of semiconductors and provide a basis of the electron device technologies.

Zusammenfassung

Eine theoretiche Behandlung des Subjekts der Oxydation auf der Si(100)-Oberfläche wird hier bekanntgemacht. Wir haben die *ab–initio*–Gesamtenergiebandstruktur– und -kraftberechnungen im Rahmen der lokalen Dichtenäherungsrechnung für den auf den Si(100)–Oberflächen adsorbierten Sauerstoff durchgeführt. Die adsorbierten Sauerstoffatome und die Si–Atome der Oberläche sind entsprechend den berechneten Kräften vollständig entspannt worden. Wir haben die folgenden Erkenntnisse gefunden: (1)Dissoziation eines O_2–Moleküls an jede beliebige Stelle der Si(100)–Oberfläche, (2)drei (meta–)stabile Stellen der adsorbierten O–Atome auf der Oberläche und (3)Durchdringen von Sauerstoffmolekülen durch die schon oxidierte Oberfläche. Eine eigentümliche Verformung von Si–Atomen und eine Volumenausdehnung des Substrats bei der Oxydation sind auch demonstreirt worden. Diese Ergebnisse geben uns eine grundlegende Kenntnis der Oxydation von Halbleitern und bieten eine Grundlage für die Technologie elektronischer Vorrichtungen.

Acknowledgments

The author is indebted Drs. A. Oshiyama and A. Ishitani for continual guidance, encouragement and supervising the present papers patiently. The author thanks Mrs. I. Hirosawa, H. Tsuda, T. Ide, and Drs. T. Mizutani, T. Tatsumi, and J. Mizuki for the fruitful discussions with their experimental point of view. His thanks are extended to Dr. S. Tsuneyuki for providing his essential ideas about the pressure–induced phase transition of the SiO_2.

The coding of the program of the force calculation is gratefully supported by Professor N. Shima, and Drs. K. Shiraishi and T. Nakayama. The author is pleased to acknowledge Drs. M. Saito, O. Sugino, S. Saito, S. Sawada, N. Hamada, and Y. Mochizuki for their useful discussions.

The English expressions in this thesis are gratefully supported by Dr. A. Oshiyama. The author is also indebted Professors A. Yoshimori and K. Cho for their careful reading of this thesis.

This work has been financially supervised and supported by H. Watanabe, Y. Matsumoto, and M. Ogawa. The present calculations have been done on SX2 at the supercomputer–center in NEC Tsukuba laboratories.

Contents

Chapter 1

Introduction

1.1 Motivation

Silicon oxidation is a familiar phenomenon in nature from ancient times and it is a popular technique for the electronic devices. Upon the oxidation of a silicon wafer, the film of the silicon dioxide (SiO_2) appears on the surface. Since the SiO_2 is a good insulator with high dielectric constant it is used in a electric circuit as a gate array or a capacitor in the memory units. In a macroscopic scale, the silicon oxidation is understood as a phenomenon in which the volume of the silicon substrate expands and then the amorphous SiO_2 is formed. More detailed informations were not required since the oxide films work well in usual electronic devices. However recent technologies of the highly integrated electronic circuits require the new technique of the formation of the ultra thin oxide films with *high quality* on the silicon substrate. (The definition of the *high quality* is not physically established yet, but it may mean that the oxide films are free from the impurities, vacancies or defects.) When the thickness of the oxide film is reduced to less than $100\mathring{A}$, the electronic and mechanical properties of the film play an important role in determining the quality of the electronic devices. These properties of the film are sensitive to its atomic structures. A fundamental knowledge of the microscopic structure of oxide films on silicon surfaces becomes very important. But unfortunately, the explicit model of the microscopic structures of the oxide films on the silicon substrates is not known yet; How do the Si and O atoms combine with each other and what is the stoichiometry of Si and O atoms

of the thin oxide film. One of the promising approach to know the answers of these questions is to investigate the oxygen reaction on silicon surfaces since it may play an important role in the determination of the structure of the oxide films in atomic scale.

Let us now review this subject from the scientific view point. It is well known that there is a lot of crystalline phase of the SiO_2, i.e. *quartz, coesite, stishovite, tridimite* and *cristobalite*, depending on temperatures and pressures.[46] None of them can fit on the silicon surfaces without a large lattice mismatch, i.e. more than 10% in average. However, the works of the transmission electron microscope (TEM) report that there are abrupt and flat interfaces between the oxide film and silicon substrate after the oxidation on the clean Si(100) surface.[1] These facts raise the following fundamental questions in addition to the technological viewpoint, i.e. **how do silicon and silicon dioxide connect to each other** and **how on earth does oxidation proceed on silicon surfaces ?** It is a challenging work to answer these questions since there are possibilities of the discoveries of new structures of SiO_2 on the silicon surfaces which are not exhibited in usual phase diagrams.

The initial oxidation is well known as a phenomenon consisting of two stages. (For example see reference.[2]) In the first stage of the oxidation, the amount of the oxygen coverage increases rapidly up to 1 mono layer (1ML) coverage: the composition of one O atom per one surface Si atom. In the next stage of the oxidation, the rate of oxidation is reduced and then the SiO_2 is formed. It is of scientific interest to clarify how do O and Si atoms combine with each other in these two stages of the oxidation. The first approach to clarify the phenomenon is to characterize the oxygen adsorption sites on the silicon surfaces. During the experiments of the oxidation, one has to keep the surface free from any contaminant which disturbs the measurement and has to control the oxygen exposure on silicon surfaces. These experimental works therefore require strict conditions of the high vacuum.

A lot of experimental works has been done to explore the phenomena in an initial stage of the oxidation on silicon surfaces. It is possible to construct suitable models of atomic geometries for the adsorbed oxygen by careful interpretation of the experimental data, i.e. the signals from the

emitted electron, reflected or transported lights, or some kinds of the diffraction patterns from the surface. But the atomic scale understanding of the phenomena is still poor because of some difficulties in experimental technique and because of lack of the knowledge of the stabilities of atomic configurations. The person who wants to propose a model of the configuration of the O and Si atoms has to examine whether nature permits the existence of the configuration or not. At this point the theoretical approach on the basis of the energetics is required. The energetics can answer the following questions; (1)What configurations of O and Si atoms are possible in nature ? (2)How much is the resulting stabilization energy ? The answers of these questions are essential for the understanding of the atomic scale structures and for the interpretation of the experimental results.

Recent progress of the super computer enables us to perform the first principles calculation for large systems on the basis of the quantum mechanics. It is well known that the local density approximation with the use of pseudopotentials is a reliable tool to obtain the stable atomic structures and the corresponding electronic states and to obtain the total energies of the condensed matters. It is also possible to propose the new atomic configurations from the theory which have not been observed yet. In this thesis we have calculated the total energies and the force on each atom of oxygen adsorbed surfaces with the use of the local density approximation. We have obtained the microscopic pictures of oxygen reactions on the Si(100) surface; i.e. *dissociation* and *adsorption* on the surface, and *penetration into the bulk*. The resulting effects upon oxygen adsorption on the silicon substrate have also been clarified, i.e. *preservation* or *destruction* of the intrinsic atomic structure of the Si(100) surface, and *volume expansion* of the substrate. It is, to our knowledge, the first microscopic calculation to visualize the microscopic phenomena of the initial oxidation of silicon. The results give us a fundamental knowledge of the silicon oxidation and a basis of the technologies of the electronic devices.

1.2 Historical survey

A great deal of works has been done to explore the atomic and electronic structures of oxygen on the silicon surfaces. The experiments have been performed in the high vacuum conditions. Meanwhile, the theoretical approaches have been done to explain the experimental works and to clarify the atomic and electronic structures of the adsorbed oxygen. However, the results of the previous results are somehow confusing because of the two reasons. One of the two is that the experimental data of the atomic structures of the O and Si atoms are indirect and then the interpretation of the data depends on the experimentalist. The other reason is that none of the previous works can give the detailed atomic structures without referring to another results. In the following, let us demonstrate how the previous results are confusing with respect to the following questions; Can the O_2 molecule adsorb on the silicon surface or not ? Which configuration is favorable for the adsorbed O atom, Si–O or Si–O–Si ? In the following five subsections, are reviewed the experimental works with several techniques which are useful for the characterization of the atomic and electronic structures on the surfaces. Next, the survey of the previous theoretical works is done. In the last subsection, we show what are the remaining problem of the oxidation.

1.2.1 EELS

Electron Energy Loss Spectroscopy (EELS) is a useful tool to know the bond configurations of the surface species. The works of the EELS were performed to determine the atomic configurations of the adsorbed oxygen on silicon surfaces at first. In the EELS study, the kinetic energy of the electrons reflected from the surface or penetrated through the sample is compared with the kinetic energy of incident electrons. The difference of these kinetic energies corresponds to the excitation energy of the electrons from surface occupied level to its unoccupied level or corresponds to the energy of local vibrational motions of the species on the surfaces.

There are two subjects of atomic configurations of oxygen on silicon surfaces. The first is the

possibility of the molecular adsorption of oxygen on the silicon surfaces. Ibach and Rowe[2] have proposed the possibility of the molecular adsorption of the oxygen on the Si(111) and Si(100) surfaces. They measured the vibrational energies of the adsorbed oxygen on the surfaces by the EELS method. Then they discussed the possible geometries of the adsorbed oxygen according to the three vibration modes with the vibrational energies 94, 130, and 175meV. They were assigned to the vibrational modes of an O_2 molecule on the surfaces. On the other hand, Nishijima et al. have proposed the coexistence of O_2 molecules and dissociated oxygen atoms on the Si(111) surface by the same experimental technique.[5] They observed the vibrational energy at 155meV, and assigned it to the stretching mode of the O=O double bond on the surface. The intensity of this vibrational loss peak weakened after the sample annealing so that they concluded that the dissociative adsorption of oxygen is favorable on the silicon surfaces in an initial stage of the oxidation. However, these works did not give us direct informations about the explicit atomic geometries of the adsorbed O_2 molecule.

The other subject is the adsorption sites of the O atoms on the Si surfaces after the dissociation of the O_2 molecule. The possibility of adsorption of the O atom on the top of the Si(100) and Si(111) surfaces was proposed by Ludeke and Koma with the EELS work.[4] They performed the EELS of electron excitation and then obtained the electronic levels which can be compared with those of the molecular orbitals of the Si–O complex. According to their work, the EELS spectrum on the Si(111) and Si(100) are identical. They have concluded that the O atom sits on top of the surface Si atom both on Si(100) and Si(111) surfaces. On the other hand, a bridge site of the adsorbed O atom, i.e. O atom on the center of the two neighboring Si atoms on the Si(111) surface, was proposed by the EELS of the excitation of the local vibrational motion by Nishijima et al.[5] They observed the energies of vibrational modes 96, 108, 123, and 155meV and assigned them to the Si–O stretching mode, the symmetric and asymmetric stretching modes of Si–O–Si complex, and the O=O stretching mode of molecular oxygen, respectively. The vibrational energies were compared with the calculated values by the valence force field method. Nishijima et al also found that the energies of the symmetric and

asymmetric vibrational modes of the Si–O–Si complex varied with increasing oxygen coverage.[5] From this fact, they proposed that the bond angle of the complex is increased upon further oxygen exposure and finally it becomes the same value of that of the α–quartz which is the most stable phase of the SiO_2. As for the Si(100) surface, Schaefer et al.[16] also reported the Si–O–Si formation by the same experimental method.

Note that the observed energies of the vibrational modes of the adsorbed oxygen in the work[5], 96, 108, 123, and 155meV, are similar to those of the another results, 94, 130, 174meV.[2] But in the former the Si–O–Si structure was proposed and in the later this structure was ruled out. This indicates that interpretations of the experimental data only with one method sometimes causes the misunderstanding of the structures. Ibach et al.[7] also pointed out that it is dangerous to use the information of the local vibrational energy as a fingerprint of the surface spices, since for example the characteristic frequencies of the Si–O and O–O single bonds fall into similar values.[7] It is therefore very inevitable to combine the several experimental methods to clarify the atomic structures.

1.2.2 XPS

The works of the X-ray Photoemission Spectroscopy (XPS) of the core levels of each atom on the oxygen adsorbed surface have also been performed. This technique is useful to understand the chemical environment around atoms. Again let us be back to the subjects of the possibilities of the molecular adsorption of the oxygen and of the atomic configurations of the adsorbed O atoms on the silicon surfaces. The O $1s$ core level shifts were observed in XPS measurements[19, 20, 26] and again the molecular and atomic forms of the adsorbed oxygen was discussed. In an initial stage of oxidation at room temperature on Si(111) and Si(100), Hollinger et al.[19] found that the O $1s$ level splits into two levels, 532 and 534eV below the Fermi level. The peaks at the 534eV disappeared after sample annealing. They assigned these levels as the emission from the stable O atom between two Si atoms on the surface and from the precursor O atom on the top site of surface Si atoms, respectively. The former agrees with the

EELS result by Nishijima et al.[5] who observed the symmetric and asymmetric vibration modes of the Si–O–Si complexes. The later agrees with the EELS results by Ludeke and Koma[4] who observed the electronic levels similar to the molecular orbitals of the Si–O. Meanwhile upon oxidation at 150K on the Si(111) surface, Höfer et al.[20] found another shift of O $1s$ peak, 530.5eV below the Fermi level instead of the peak of 534eV by Hollinger et al. Then this shifted peak disappeared after sample annealing. They assigned it as a molecular adsorbed oxygen. This results seems to support the results of EELS by Nishijima et al.[5] who observed the O=O stretching mode. The XPS of O $1s$ level thus complements the results of the EELS. However, the results still give us indirect informations about the atomic configurations of O and Si atoms. That is the reason why the approach on the basis of the energetics is required.

In addition to the core level of the O atoms, informations of the Si core level are useful to know the coordination numbers of the O atoms around Si atoms.[18, 25] Because when O atom approaches Si atom the charge transfer from Si to O atoms occurs and that cause the chemical shift of the Si $2p$ levels. Hollinger and Himpsel observed the chemical shift of Si $2p$[18], and they discussed the coordination numbers of O atoms around Si atoms. They proposed the possibility of the variation of the oxygen coordination numbers from 1 to 4 in an initial stage of the oxidation and in the oxide film.

1.2.3 UPS

To understand the chemical bonds of the Si and O atoms the knowledge of the energy levels of valence electrons is important. The Ultra violet Photoemission Spectroscopy (UPS) is a useful tool to know the density of state of the valence electrons. The stable site of the adsorbed O atom and the coexistence of the molecular oxygen were again discussed in these works.[17, 18, 20] The density of states of valence electrons were measured by the UPS by Hollinger and Himpsel.[18] The appearance of typical three peaks after oxygen adsorption and sample annealing was reported on the Si(100) surface. The first two peaks in increasing energy level were assigned as two O $2p$ bonding levels and the third peak was assigned nonbonding orbital

of the Si–O–Si complex. The result was derived from the theoretical work of the bulk SiO_2.[45] This result suggests the Si–O–Si formation after the oxygen adsorption which agrees with the work of EELS by Nishijima et al.[5] Meanwhile, the valence band structure of the molecular adsorption of oxygen was also reported by Höfer et al.[20] They measured the photoemission from the oxidized Si(111) surface at 150K. In the beginning of the experiments, two peaks appeared at about 2 and 4eV below the Fermi level. These peaks gradually disappeared when they continued the experiments. The intensities of the two peaks depended on the polarization directions of the incident light. They concluded the origin of the peaks as a oxygen precursor state on the Si(111) surface and finally proposed the model of the laying O_2 molecule on the bridge site between two surface Si atoms.

1.2.4 SEXAFS

The detailed structure of the local atomic configuration of the Si and O atoms on the surface was investigated with use of the Surface Extended X-ray Absorption Fine Structure (SEXAFS) method by Incoccia et al.[38] This method is based on the interference effect of the intensities of the photoexcited electrons with respect to the kinetic energies of the photoelectrons. They used the polarized light and then they carefully interpreted the polarization effect on the interference of photoelectrons. According to the polarization dependency of the data of the oxygen adsorbed Si(100) surface, the existence of the Si–O–Si complex was again suggested and it was also proposed that the Si–Si line of the complex is tilted to the surface. But unfortunately only this local configuration could be determined from this experimental results.

1.2.5 Other experiments

As shown before, it is hard to obtain the concrete evidence of the detailed structures of the adsorbed oxygen on the silicon surfaces. There are works which tried to clarify the atomic configurations of oxygen adsorbed silicon surface with use of another experimental techniques. Let us finally survey these experimental works. Keim et al.[25] performed the

reflectivity measurement on the oxidized Si(100) surface. In this experiment, the enhancement of the difference of the reflectivity $\Delta R/R$ appears when the incident photon energy corresponds to the energy gap between the occupied and unoccupied levels of the electronic states. They referred the theoretical results for the clean Si(100) surface by Pollmann et at.[22] and discussed the origins of the peaks of the $\Delta R/R$. Upon oxidation within 1ML oxygen coverage, one of the peaks of the $\Delta R/R$ disappeared prior to the disappearance of other peaks. This peak was assigned as the electron transition between the occupied and unoccupied surface states which come from the surface dangling bonds. From this results they proposed that the most favorable sites of the oxygen in an initial stage of the oxidation are the dangling bonds of the surface Si atoms.

The works of the scanning tunneling microscopy (STM) were done to explore the kinetics of the oxidation on the Si(111) surface.[23, 24] In the works of the STM the tunneling currents between the surface and very sharp tip are monitored and the local density of state of the electron is measured in the space resolution of the atomic scale. Tokumoto et al.[23] showed the real space image of the local density which were integrated to the extent of the energy region from the Fermi level to 1eV below it. They found that upon the oxidization on the Si(111) surface the image of the top most Si atoms disappears earlier than the image of the other surface atoms. This result suggests that the O atom approaches and sits on the top silicon atom at first.

In addition to the static oxygen on the surface, the mobile states of the oxygen molecule on the silicon surface were also observed. Rechtien et al.[6] performed he molecular scattering experiments and they suggested that the charged molecular states O_2^- appears during the oxygen collision on the Si(100) surface.

1.2.6 Theoretical works

In addition to the experimental works, the theoretical approaches were done for the subjects of the oxidation on silicon surface. The cluster model was adopted to mimic the surface silicon, and

the electronic states of the adsorbed oxygen were investigated.[10, 13, 14, 15] Goddered. *III* et al.[10] suggested the model of the O_2 molecule which is laying on the surface. It is called as peroxy radical model. According to the results, the single bond network of $Si_{surface}$–O–O is achieved and one electron is in the O p_x orbital which expands in parallel to the surface and normal to the O_2 bond axis. But they did not confirm the stability of this structure yet. On the other hand, the stability of the atomic oxygen on the Si(100) and Si(111) surfaces was investigated by Russo et al.[13] and by Batra et al.[14] The results says that on both surfaces the most stable site for atomic oxygen is a bridge site between the two (three) Si atom on the Si(100) (Si(111)) surface. But the relaxation of the substrate Si atoms was not taken into account yet and the mechanisms of the oxygen dissociation was not clarified. Chen et al.[11] and Ciraci et al.[12] performed the band–structure calculation of the valence electronic states for the oxygen adsorbed Si(111) surfaces to explain the experimental data form the UPS. These calculation was based on the tight–binding method with the realistic parameters which were constructed from the results of the first principles calculation of the bulk SiO_2. They concluded that the O_2 adsorption is unfavorable since the calculated density of state did not agree with the UPS results. Meanwhile the DOS of oxygen atoms on bridge site on the Si(111) surface agreed with the UPS data. Their results indicate that on the Si(111) surface the Si–O–Si complexes are formed upon oxidation. Recently, Smith et al.[15] calculated the total energies of adsorbed O atom and O_2 molecule on the Si(100) surface with use of the cluster model. They considered the reconstruction of the surface Si atoms. They expressed that the bridge site of the Si(100) surface is stable for the adsorbed O atom. They also calculated the total energy surface of the O_2 molecule on the reconstructed Si(100) surface with fixed O–O bond length and the fixed tilt angle of the molecular axis. Then they found a local minimum site of the total energy for the O_2 molecule. They therefore proposed that this corresponds to the metastable site for the O_2 molecule. However these results are questioned from our present results because they did not consider the stretching of the bond length and tilting of the molecular axis of the oxygen and they did not calculate the forces on each atom. Only after the force calculation it is possible

to discuss the stability of the adsorbed molecule.

1.2.7 Problems in previous works

Now we have quickly surveyed the previous works for the clarification of the oxygen reaction on silicon surfaces. The possible models about local atomic configurations of adsorbed oxygen on silicon surfaces can be obtained from the experimental and theoretical works. However the results thus raise somewhat confusing remarks. Some people emphasized the existence of the O_2 molecule on silicon surfaces and the others do not. Some people proposed the Si–O configuration for the adsorbed O atom and the others proposed the Si–O–Si configuration. As we said before, the confusion of the previous works is understood by following two reasons; (1)The experimental results which show the atomic configurations of adsorbed oxygen are indirect so that one needs the interpretation of the experimental data. (2)None of the previous works can explain the detailed atomic configuration without referring the other experimental and theoretical works. Now the following fundamental questions still remain.

1. **Where is the most stable site for an O_2 molecule or an O atom on the surfaces ?**

2. **What are the mechanisms of the dissociation of the molecular oxygen if it occurs ?**

3. **How does an oxygen molecule penetrate through oxidized surface when the oxidation continue ?**

4. **How are the oxide films formed on the silicon surfaces ?**

The detailed answers to these questions are not fully elucidated yet. On the other hand the approach on the basis of the energetics independent on other works therefore give us the fundamental understanding of the oxidation.

1.3 The structure of the Si(100) surfaces

Before describing our present results, we have to describe why we have chosen the Si(100) surface as a subject. When one cleaves the silicon crystal, the Si atoms of the surface lose some of the neighboring atoms which made the covalent bonds in the bulk. Then if the surface atoms stay in the ideal positions as in the bulk, each atom has dangling bonds that cause an increase of the total energy. However on real surfaces, each atom on the surface is displaced and makes the new covalent bonds with its neighbors. The resulting structures of the surfaces show reconstructions which have larger periodic boundaries than that of the ideal surfaces. First of all the Si(111) surfaces have been investigated since these surfaces can be easily obtained by cleaving the silicon crystal in vacuum and the surface structure is stable during the measurements. On the other hand the Si(100) surfaces are rather unstable than Si(111) surfaces. The sophisticated experimental studies on the Si(100) surfaces are therefore rather difficult than that on the Si(111) surfaces. However, recent progress of the techniques of the sample preparation in vacuum enables us to investigate its properties, i.e. phase transition at several temperatures, chemical reactions with other atoms and molecules, etc. These properties of the Si(100) surfaces raise the fundamental interest of condensed matters physics. The Si(100) surfaces are also important from the technological point of view. The electronic circuits are usually fabricated on the Si(100) surfaces because of the biggest crystal growth rate of the surface among other silicon surfaces. The oxide film formations on the Si(100) surfaces is a key technique of the electronic devices.

Let us review the microscopic structure of the Si(100) surface. Fig. 1-1(a) shows the schematic diagram of the top view of the surface structure of the silicon crystal cleaved at the (100) crystallographic plane. The circles of the biggest size denote the top most Si atoms and the circles of the middle and the smallest sizes denote the second and third layer Si atoms, respectively. On the realistic surface, the reconstruction of the surface Si atoms occurs. The neighboring surface Si atoms bind each other and make the dimers shown in Fig. 1-1(b). After

the reconstruction, the lateral periodic boundary in the $(01\bar{1})$ direction is extended 2 times longer than primitive period of the bulk. Meanwhile the period in the (011) direction is kept same as the primitive one. Then we call it as a 2×1 periodic boundary condition or simply call this surface as the Si(100)2×1 surface. The surface Si atoms still preserve the one dangling bond per atom which makes the surface localized states of electron. There are issues about the detailed structure of the Si(100) surfaces[43, 44]; Are the dimers buckled or not ? What is the favorable periodic boundary of the buckling dimers if so ? How are the second and third layer Si atoms displaced ? Can theory explain the electronic structure of the surface when the atomic structure is clarified ? Some experimental and theoretical works show inconsistent results and this problem becomes confusing issues. However the difference of the calculated total energies per dimer in several structures is within 0.1eV. In addition to that, the surface Si atoms show peculiar distortions after the oxygen adsorption. (We will show the results in chapter 3.) We therefore believe that the resulting geometries of adsorbed oxygen do not depend on the details of the structure of the Si dimers on the clean Si(100) surface. In this work we have investigated the oxygen reaction on the Si(100) surface with use of the model of the symmetric dimers for the clean surface.

1.4 Organization of present thesis

In chapter 2, the details of our calculation are shown. We report the derivation of the total energy and forces within the local density approximation. The formalisms of use of the localized orbital basis set are also described here. In the last section of the chapter 2, we show the evidence of the validity of our present calculation by showing the reproduction of the well established results.

In chapter 3, we report the calculated results. The atomic configuration is optimized until it approaches to the stabilized structure according to the calculated forces. (We call this calculation as a **geometry optimization** in this thesis.) In the first section, we show the

O_2 reaction on Si(100) surfaces. The results of the geometry optimization of the O_2 molecule and surface Si atoms are shown. In the second section, we show the results of the geometry optimization of the O atoms and surface Si atoms on the Si(100) surface. The result gives (meta)stable sites of the adsorbed O atom. In the third section, the vibrational energy and electron density of states have been calculated in the (meta)stable geometries and they have been compared with the experimental results available. In the last section of the chapter 3, the results of penetration and adsorption of the oxygen on the 1ML oxidized Si(100) surface is demonstrated. The new structures which are similar to the crystalline phase of the SiO_2 appear.

Finally in the last chapter, we discuss the general phenomenon of oxidation of silicon, and discuss the theoretical methods necessary for further understanding.

Chapter 2

Calculation

2.1 Total energy and forces within the local density approximation

Hohenberg and Kohn[29] proved that the total energy of the ground state of manybody system can be determined as a function of a charge density of electrons. In this thesis the pseudopotentials are used to mimic the interaction of nuclei and core electrons with valence electrons so that the total energy E of a periodic system is written as

$$E = \sum_{n,k}^{occup} \int \psi^*_{nk}(\mathrm{r})(-\nabla^2 + V^{ps}_{lo}(\mathrm{r}))\psi_{nk}(\mathrm{r})d\mathrm{r} + \sum_{n,k}^{occup} \int\int \psi^*_{nk}(\mathrm{r}')V^{ps}_{nl}(\mathrm{r}',\mathrm{r})\psi_{nk}(\mathrm{r})d\mathrm{r}'d\mathrm{r} + \frac{1}{2}\int \rho(\mathrm{r})V_H(\mathrm{r}) + \frac{1}{2}\sum_{\mathrm{R},\mathrm{R}'} \frac{Z_{\mathrm{R}}Z_{\mathrm{R}'}}{|\,\mathrm{R}-\mathrm{R}'\,|} + E_{xc}(\rho) \quad . \tag{2.1}$$

In this equation, the wave functions of valence electrons are expressed as $\psi_{n,k}(\mathrm{r})$ in which n and k denote band index and wave number, respectively. The $V^{ps}_{lo}(\mathrm{r})$ and $V^{ps}_{nl}(\mathrm{r}',\mathrm{r})$ represent the local and nonlocal part of the norm–conserving pseudopotentials.[30] The first and second terms indicate the kinetic energies plus interactions with the nuclei and core electrons of the valence electrons. The third term expresses the static Coulomb potential between valence electrons. The fourth term is Coulomb repulsion between the ions. The R and Z mean the atomic coordinates and the valence charges of positive ions, respectively. The last term is the

exchange correlation energy of the valence electrons. The charge density $\rho(\mathbf{r})$ is given as

$$\rho(\mathbf{r}) = \sum_{n,k}^{occup} \mid \psi_{nk}(\mathbf{r}) \mid^2 \ , \tag{2.2}$$

in which the $\sum^{occup}$ means the summation over the occupied states. The $V_H(\mathbf{r})$ is the Hartree potential which is given as

$$V_H(\mathbf{r}) = \int \frac{\rho(\mathbf{r}')}{\mid \mathbf{r} - \mathbf{r}' \mid} d\mathbf{r}' \ . \tag{2.3}$$

The $E_{xc}(\rho)$ is the exchange correlation energy which is given as

$$E_{xc}(\rho) = \int \rho(\mathbf{r}) \varepsilon_{xc}(\ \rho(\mathbf{r})\ ) d\mathbf{r} \ , \tag{2.4}$$

where $\varepsilon_{xc}(\rho)$ is expressed as a functional of the density of the valence electrons in the analytic form[31] which is fitted to the numerical results[32].

In this thesis we have used the norm–conserving nonlocal pseudopotentials which simulate the effects of the nuclei and core electrons to the valence electrons. The pseudopotentials are same as those which have been used for the previous work by Oshiyama and Saito.[27, 28] They constructed the norm–conserving nonlocal pseudopotentials from their results of all electron calculations of the Si and O atoms within the local density approximation following the method by Bachelet–Hamman–Schlüter[30]. The validity of the application of the pseudopotentials to the subject of the oxygen reaction on the Si(100) surface has been confirmed which will be exhibited in subsection 2.2.

According to the variational principle, the ground state of the system is achieved when the gradient of the total energy with respect to the wave function is zero. This fact derives the Eular's equation which is given as

$$H\psi_{nk}(\mathbf{r}) = \varepsilon_{nk}\psi_{nk}(\mathbf{r}) \ , \tag{2.5}$$

in which the H is written as

$$H = -\nabla^2 + V_{lo}^{ps}(\mathbf{r}) + V_{nl}^{ps}(\mathbf{r}', \mathbf{r}) + V_H(\mathbf{r}) + \mu_{xc}(\rho) \ . \tag{2.6}$$

In the equations (2.5) and (2.6), the ε_{nk} is the Lagrange's undetermined multipliers and the μ_{xc} is given as

$$\mu_{xc}(\rho) = \frac{\delta \rho \varepsilon_{xc}(\rho)}{\delta \rho} \quad . \tag{2.7}$$

The equation (2.5) is well known as the Kohn Sham equation[29] which takes the form of the Shrödinger equation with the effective hamiltonian H of equation (2.6), and the ε_{nk} corresponds to the energy levels of the eigenfunctions ψ_{nk}. With use of the equations (2.2) $\sim$ (2.6), one can rewrite the total energy E as

$$E = \sum_{n,k}^{occup} \langle \psi_{nk} \mid H \mid \psi_{nk} \rangle - \frac{1}{2} \int V_H(\mathbf{r}) \rho(\mathbf{r}) d\mathbf{r} + \int \rho(\mathbf{r}) \{ \varepsilon_{xc}(\rho(\mathbf{r})) - \mu_{xc}(\rho(\mathbf{r})) \} d\mathbf{r} + \frac{1}{2} \sum_{\mathbf{R},\mathbf{R}'} \frac{Z_{\mathbf{R}} Z_{\mathbf{R}'}}{\mid \mathbf{R} - \mathbf{R}' \mid} \quad . \tag{2.8}$$

Forces $\mathbf{F}_\tau$ are given as the negative gradients of the total energy E with respect to the atomic coordinates τ. At first let us show the negative gradients of the second and the third terms of the equation (2.8) which are given as follows:

$$-\frac{\delta}{\delta \tau} \left(-\frac{1}{2} \int V_H(\mathbf{r}) \rho(\mathbf{r}) d\mathbf{r} \right) = \int \frac{\delta V_H(\mathbf{r})}{\delta \tau} \rho(\mathbf{r}) d\mathbf{r} \quad , \tag{2.9}$$

and

$$-\frac{\delta}{\delta \tau} \int \rho(\mathbf{r}) \{ \varepsilon_{xc}(\rho(\mathbf{r})) - \mu_{xc}(\rho(\mathbf{r})) \} d\mathbf{r}$$

$$= -\int \frac{\delta \rho(\mathbf{r})}{\delta \tau} \frac{\delta \{ \rho(\mathbf{r}) \varepsilon_{xc}(\rho(\mathbf{r})) \}}{\delta \rho(\mathbf{r})} d\mathbf{r} + \int \frac{\delta \rho(\mathbf{r})}{\delta \tau} \mu_{xc}(\rho(\mathbf{r})) d\mathbf{r} + \int \rho(\mathbf{r}) \frac{\delta \mu_{xc}(\rho(\mathbf{r}))}{\delta \tau} d\mathbf{r}$$

$$= \int \rho(\mathbf{r}) \frac{\delta \mu_{xc}(\rho(\mathbf{r}))}{\delta \tau} d\mathbf{r} \quad . \tag{2.10}$$

These are derived from the equations (2.3) and (2.7). Since the norm of the wave function $\psi_{nk}(\mathbf{r})$ is constant with regard to the atomic coordinates we can also note that

$$\frac{\delta}{\delta \tau} \int \psi_{nk}^*(\mathbf{r}) \psi_{nk}(\mathbf{r}) d\mathbf{r} = 2 Re \langle \frac{\delta \psi_{nk}}{\delta \tau} \mid \psi_{nk} \rangle = 0 \quad . \tag{2.11}$$

With use of previous equations (2.9) $\sim$ (2.10) we can obtain the force on atom τ as

$$\mathbf{F}_\tau = -\frac{\delta E}{\delta \tau} = -\sum_{n,k}^{occup} \langle \psi_{nk} \mid \frac{\delta H}{\delta \tau} \mid \psi_{nk} \rangle + \int \frac{\delta V_H(\mathbf{r})}{\delta \tau} \rho(\mathbf{r}) d\mathbf{r} + \int \rho(\mathbf{r}) \frac{\delta \mu_{xc}(\ \rho(\mathbf{r})\ )}{\delta \tau} d\mathbf{r}$$

$$+ \sum_{\mathbf{R}} \frac{Z_\tau Z_{\mathbf{R}}}{\mid \tau - \mathbf{R} \mid^3} (\tau - \mathbf{R}) - 2Re \sum_{n,k}^{occup} \langle \frac{\delta \psi_{nk}}{\delta \tau} \mid H \mid \psi_{nk} \rangle \ .$$

By substituting the equation (2.6) into the first term of the force and applying the result of the equation (2.11) to the last term, we can obtain the final expression of the force as

$$\mathbf{F}_\tau = -\sum_{n,k}^{occup} \langle \psi_{nk} \mid \frac{\delta V_{lo}^{ps}}{\delta \tau} + \frac{\delta V_{nl}^{ps}}{\delta \tau} \mid \psi_{nk} \rangle + \sum_{\mathbf{R}} \frac{Z_\tau Z_{\mathbf{R}}}{\mid \tau - \mathbf{R} \mid^3} (\tau - \mathbf{R})$$
$$-2Re \sum_{n,k}^{occup} \langle \frac{\delta \psi_{nk}}{\delta \tau} \mid H - \varepsilon_{nk} \mid \psi_{nk} \rangle \ . \tag{2.12}$$

If the wave functions $\psi_{nk}(\mathbf{r})$ are the true solutions of the Kohn-Sham equation (2.5), the last term of the equation (2.12) vanishes. This fact is known as the Hellmann–Feynman theorem and the first and second terms in the equation (2.12) constitute the Hellmann–Feynman force and the last term is called as the correction term.

Instead of the true solutions, the linear combinations of the Bloch wave functions $\{\phi_\alpha^k(\mathbf{r})\}$ consisting of the well–known functions are used to express the valence wave functions as,

$$\psi_{nk}(\mathbf{r}) = \sum_\alpha C_\alpha^{nk} \phi_\alpha^k(\mathbf{r}) \ . \tag{2.13}$$

The Kohn Sham equation (2.5) therefore becomes a secular equation with respect to the coefficients $\{C_\alpha^{nk}\}$. The equation is written as

$$\sum_\beta H_{\alpha\beta}^k C_\beta^{nk} = \varepsilon_{nk} \sum_\beta S_{\alpha\beta}^k C_\beta^{nk} \ , \tag{2.14}$$

in which

$$H_{\alpha\beta}^k = \langle \phi_\alpha^k \mid H \mid \phi_\beta^k \rangle \ , \quad \text{and} \quad S_{\alpha\beta}^k = \langle \phi_\alpha^k \mid \phi_\beta^k \rangle \ .$$

The effective hamiltonian H is obtained by substituting a guessed charge density $\rho(\mathbf{r})$ into the equations (2.3) and (2.4) and then substituting these two equations into the equation (2.6), and then the secular equation (2.14) is solved. The new $\rho(\mathbf{r})$ is obtained according to the equation (2.2). The series of these calculations is performed iteratively since the convergence of the $\rho(\mathbf{r})$ is achieved.

With use of the basis set $\{\phi_\alpha^k(\mathbf{r})\}$ the force in the equation (2.12) is rewritten as

$$\mathbf{F}_\tau = -\int \rho(\mathbf{r}) \frac{\delta V_{lo}^{ps}}{\delta \tau} d\mathbf{r} - \sum_{k,\alpha,\beta} N_{\alpha,\beta}^k \int\int \phi_\alpha^{k*}(\mathbf{r}') \frac{\delta V_{nl}^{ps}(\mathbf{r}', \mathbf{r})}{\delta \tau} \phi_\beta^k(\mathbf{r}) d\mathbf{r}' d\mathbf{r}$$
$$+ \sum_{\mathbf{R}} \frac{Z_\tau Z_{\mathbf{R}}}{|\tau - \mathbf{R}|^3} (\tau - \mathbf{R}) - 2Re \sum_{k,\alpha,\beta} N_{\alpha,\beta}^k \langle \frac{\delta \phi_\alpha^{k*}}{\delta \tau} \mid H - \varepsilon_{nk} \mid \phi_\beta^k \rangle \ , \tag{2.15}$$

in which

$$N_{\alpha,\beta}^k = \sum_n^{occup} C_\alpha^{nk*} C_\beta^{nk} \ .$$

According to the secular equation (2.14) the leaving term which includes the gradient of the coefficients C_α^{nk} with respect to the τ vanishes:

$$-2Re \sum_{\alpha,\beta,n,k}^{occup} \frac{\delta C_\alpha^{nk*}}{\delta \tau} C_\beta^{nk} \langle \phi_\alpha^{k*} \mid H - \varepsilon_{nk} \mid \phi_\beta^{nk} \rangle = 0 \ .$$

When plane wave basis set is used for the wave function expansion, the correction term in the equation (2.15) becomes zero because of an independence of the plane wave basis on the atomic coordinates. Meanwhile when the atomic localized basis set is used, we have to calculate the correction term because of the dependence of the localized basis on the atomic coordinates and of the same magnitude of the correction term as the Hellmann–Feynman force.[27] The wave functions of the valence electrons of the O atom are compact and a volume of the unit cell of the surface, i.e. repeating slab, is large. When one uses the plane wave basis set for the wave function expansion in such a case, the huge number of plane waves is required to obtain the well converged total energy and stable atomic configurations. In this work we have therefore chosen the gaussian orbitals to reduce the size of the basis and then to perform the efficient

calculation. The basis set $\{\phi_\alpha^k(\mathbf{r})\}$ is obtained as the Bloch sum of the gaussian orbitals,

$$\phi_\alpha^k(\mathbf{r}) = \frac{1}{\sqrt{N}} \sum_{\mathbf{L}} e^{i\mathbf{k}\cdot\mathbf{L}} g_\alpha(\mathbf{r} - \tau_\alpha - \mathbf{L}) \quad . \tag{2.16}$$

The $\mathbf{L}$ denote the lattice vectors and the N is a number of them. The $g_\alpha(\mathbf{r})$ denotes the gaussian localized orbital with the angular momentum l_α and exponent a_α,

$$g_\alpha(\mathbf{r}) = r^{l_\alpha} e^{-a_\alpha r^2} Y_{m_\alpha}^{l_\alpha} \quad ,$$

where the $Y_{m_\alpha}^{l_\alpha}$ is the spherical harmonics. The calculated results are more accurate than those with insufficient number of the plane waves.

2.2 Confirmation of the validity of present gaussian basis set

We have used the localized gaussian orbitals for the wave function expansion. The exponents of the basis are: 0.18, 0.44, and 1.30 for Si s; 0.18, and 0.55, for Si p; 0.2812, 1.0996, and 4.4573 for O s; and 0.2213, 1.0694, and 5.5000 for O p. These gaussian orbitals have been obtained to fit the pseudo–wave functions in constructing the norm conserving nonlocal pseudopotentials. These basis set and the pseudopotentials enable us to reproduce the well established results. This fact guarantees our previous calculation. In this chapter we show the calculated results for the silicon bulk and surface, the α–quartz, and the O_2 molecule.

2.2.1 The silicon bulk and surface

We have calculated the total energy of the silicon crystal with changing lattice constants. The silicon crystal has the diamond structure which has the T_d symmetry. Considering the T_d symmetry, 10 k points in the irreducible part of the first Brillouin zone are used for the momentum space integration. Eight real mesh points per Si–Si bonds are adopted for the first Fourier transformation. The calculated total energies are shown in Fig. 2-1 as a function of the lattice constants. The optimized lattice constant 10.29a.u. has an error of 2% with the

experimental results. From this result, we can estimate the bulk modulus κ_v which is defined as

$$\kappa_v = \Omega \frac{\partial^2 E}{\partial \Omega^2} \mid_{\Omega=\Omega_0} \quad ,$$

where the Ω is a volume of the unit cell and the Ω_0 is the volume at the total energy minimized lattice constant. The curve of the total energies in Fig. 2-1 has been fitted as a parabolic function of the volume by the least square method. The resulting bulk modulus is 1.0Mbar which has an error of 10% with the experimental value. This is the reasonable error of the local density approximation.

We have next applied the gaussian basis set to the Si(100) surface. We have compared the total energies of the ideal surface with that of the reconstructed surface. (See Figs. 1-1(a) and (b).) We have optimized the Si dimer within the restriction of the symmetric model. The calculated band structure of the reconstructed surface shows the metallic feature and the total energy is lower about 1.6eV per dimer than the total energy of the ideal surface. These results agree with the previous calculation with use of the plane wave basis set.[35] Although it is of interest to ask whether the dimer is buckled or not, we have not perform the geometry optimization of the tilt angle of the dimer because, as mentioned in section 1.3, the buckling of the dimer does not affect the stable geometry of the adsorbed oxygen.

2.2.2 The α–quartz

We have optimized the lattice constant of the α–quartz using these gaussian basis set. There are three SiO_2 complexes in the hexagonal unit cell. Fig. 2-2 shows the atomic configuration of the α–quartz.[53] The relative atomic position and the ratio 1 : 1.100 of the lengths of the "a" and "c" axis of the hexagonal unit cell are fixed during the optimization. Although we can not reproduce the correct bulk modulus within this restriction, we can reproduce the lattice constant which minimizes the total energy. Fig. 2-3 shows the total energy curve with varying lattice constant. The calculated lattice constant, 9.48 a.u. for the "a" axis, has an error of 2% with the experimental values and resulting cohesive energy 1.68Ry per SiO_2 shows a good

agreement with the well converged plane wave basis results.[54]

2.2.3 The O_2 molecule

In this thesis all calculations have been done under the periodic boundary conditions. Upon oxygen adsorption on the surface, oxygen molecules or atoms are repeating on the surface. We therefore have to confirm whether interaction between adsorbates is negligible or not under the periodic boundary conditions. We have performed the band calculation of the repeating O_2 molecules with use of the local spin density approximation. We have adopted the three dimensional periodic boundary condition corresponding to the 1 × 1 period of the Si(100) surface in lateral directions and to the 8 layers thickness of the Si slab in normal direction. Then, in each unit cell, an O_2 molecule has been placed on the center of the unit cell with its axis parallel to the normal direction. We have concluded that the period of the unit cell is large enough since the calculated electronic energy levels show no dispersions in the k space. The calculated spin state is triplet which is consistent to the feature of the molecular orbital.[52] Although the optimized O-O length 1.3$\mathring{A}$ is 8% larger than previous value[52] we believe this does not affect the qualitative results of present calculation. We have estimated the binding energy E_B per O atom of the O_2 molecule. The E_B is obtained from following equation

$$E_{O_2} + 2E_B = 2E_O \quad ,$$

where E_{O_2} and E_O mean the total energies of the O_2 molecule and the O atom, respectively. The resulting value of E_B is 5.5eV.

2.3 The conditions of the present calculations

The compact nature of the oxygen orbitals requires a careful treatment of the real space mesh points in the fast Fourier transformation. Indeed the real space mesh points with the interval of 0.26 a.u. have been adopted. The geometry optimization has been performed to obtain the total-energy minimized geometries by requiring that the force acting on each atom

is reduced to typically less than 10^{-2}Ry/a.u. We perform the self-consistent calculation to obtain the well converged electronic states at each atomic configuration. The trajectory of each atomic coordinate is therefore on the adiabatic surface during the geometry optimization. When the configuration is close to the total energy minimized structure and the optimization is continued, the calculated forces start to oscillate in opposite directions with the absolute values of 10^{-2}Ry/a.u. The fact indicates that the atomic geometry is in the vicinity of the (meta)stable structure and then we finish the geometry optimization.

One of the methods to treat the oxygen reaction on the silicon surfaces is to use the large cluster geometries which mimic the silicon surface. But it is well known that this method is not free from the problem of the magic number effect of the silicon cluster.[34] We have therefore chosen the band structure calculation. On a surface, there are periods in the lateral directions but not in the normal direction, i.e. half of the system is an infinite solid and the other is a vacuum. However, the band calculation of the three dimensional systems can be applied to the surface problem when one uses *repeating slab geometries* in which the periodic boundary in the surface normal direction is adopted. The resulting unit cell corresponds to the super lattice consisting of a slab and a vacuum region. When we take a thin slab or an insufficient vacuum region in a unit cell, the electronic states on both sides of the slab interact each other and then the resulting electronic states have no realistic features of surface states. We therefore need to choose the sufficient thicknesses of the slab and the vacuum region. Indeed we have performed the total energy calculation of a slab with varying thickness of the vacuum region and confirmed that the vacuum corresponding to 8 layers Si slab is sufficient to obtain the well–converged value of the total energy. Then, we have also confirmed that the (meta)stable atomic geometry obtained for a slab with the 4 Si layers is still stable when the thickness of the slab is increased to 8 Si layers in all calculations in this thesis. Thus this method works well when the calculations of the electronic state and the total energies of the surfaces is performed with sufficient thicknesses of the slab and vacuum region. (See another example of the repeating slab method in reference [35].)

Chapter 3

Energetics of initial oxidation

Before describing the details of the initial oxidation on the Si(100) surface, we have to say what geometry and periodic boundary condition have been imposed to simulate the Si(100) surface. As we introduced in section 1.3, there are several models for the reconstructions of the Si(100) surfaces in consideration of the buckling of the dimers. However, the differences of the total energies among the models are less than 0.1eV per dimer.[43, 44] We therefore believe that final structures of the adsorbed oxygen are not sensitive to the detailed structures of the Si dimers on the clean Si(100) surface. Before oxygen adsorption, the surface Si atoms are fully optimized according to the calculated forces within the restriction of the symmetric dimer model. For the calculation of initial oxidation, we have adopted the following conditions which are sufficient to know the oxygen reactions on the Si(100) surface. The 2 × 1 and occasionally 2 × 2 lateral periodic boundary conditions are imposed for the slab calculation. These boundaries and the corresponding surface Brillouin zones are shown in Fig. 3-2. Eight k-points in the first Brillouin zone of the 2 × 1 unit cell are chosen for the momentum space integration, which are shown as dots in Fig. 3-2. Meanwhile the surface normal wave number k_z is fixed to zero. In each unit cell of the surface we put one O_2 molecule (or one O atom). During the optimization the two surfaces of the slab are kept equivalent with respect to the 180° rotation around the (011) axis, i.e. C_2 symmetry. (Fig. 3-1 shows the position of the rotation axis.) Since we neglect the spin–orbit interactions of the electrons, the states with k and -k are related by time reversal symmetry and the irreducible part of the first Brillouin zone

is the half of the whole. In addition to that, the C_2 symmetry reduces the irreducible part to the quarter of the whole so that we can reduce the calculation time of the momentum space integration.

In the following four sections we describe the results of our present calculations. In section 3.1, we show the dissociation of the O_2 molecule at almost all sites of the Si(100) surface. The mechanism of the dissociation of the O_2 molecule is understood as the electron transfer from the surface dangling bonds to the molecular antibonding π orbitals. In section 3.2, we show three (meta)stable sites of the adsorbed O atoms which preserve or destroy the dimer structure of the Si(100) surface. The adsorption site of an O atom depends on which site the preceding molecule dissociates. In section 3.3, we show the comparison of our results with the experimental data. The most stable geometry shows good agreements with the experiments. In the last section 3.4, we demonstrate that the further oxidation is still exothermic in spite of the volume expansion of the oxidized layers.

3.1 Dissociation of an O_2 molecule on the Si(100) surface

We have adopted the periodic slab geometries consisting of 4 Si layers and vacuum corresponding to 8 Si layers. The 2 × 1 lateral boundary condition has been imposed. We have placed O_2 molecules on equivalent sites on both sides of the slab. The four sites on the Si(100) surface, marked A, B, C, and D in Fig. 3-3, have been chosen as initial target areas of the adsorbed O_2 molecule. We have performed the geometry optimization of the adsorbed O_2 molecule and the surface Si atoms on each site of the four: A∼D. These four sites cover almost all possibilities of the adsorption of the O_2 molecule on the Si(100) surface. To achieve the total energy minimized geometries we have to optimize the orientation of the axis of the O_2 molecule with respect to the surface as well as its bonding length. For the efficiency of the geometry optimization we have chosen initial molecular orientations as follows; (1)On the site A, the molecule is placed with its axis normal to the surface, and (2)on each site of B, C, and

D, the molecule is placed with its axis tilted by 45° to the surface and the azimuthal angle of the molecular axis is 45° from the bond axis of the Si dimers. Before the optimization, the initial height of the center of the O_2 molecule is assumed to be $2.4\mathring{A}$ above the surface dimer. The height is twice as long as the bond length of the O_2 molecule. Then the two O atoms and the top–layer Si atoms are fully relaxed during the optimization according to the calculated forces toward the total energy minimized geometries.

On the site A, just above the dimer, the O_2 molecule dissociates. (See Fig. 3-4) The following figures show one of the two equivalent sides of the slab. Dotted and open circles mean the O and the Si atoms, respectively. For the same kind atoms, the atoms of the larger circles are closer to the reader than those of smaller circles. The two arrows in Fig. 3-4 mean the calculated forces on the two O atoms: the upper one is 0.137Ry/a.u. and the lower one is 0.085Ry/a.u. The Si dimer and the O_2 molecule are located in the (011) plane. The contour map in Fig. 3-4 means the charge density in the plane. The charge density shows a nodal feature at the center of the O_2 molecule and shows no maximums at the positions of the dangling bonds of the surface Si atoms. The result means the electron transfer which occurs from the dangling bonds of the Si dimer to the antibonding π orbitals of the O_2 molecule. The electron transfer results in the dissociation of the O_2 molecule on the site A.

On the site B, between the neighboring two dimers, the O_2 molecule lies on the surface with its axis normal to the bond axis of the dimer. The sequence of the geometry optimization is shown in the series of the pictures in Fig. 3-5. Again the arrows mean the calculated forces. Two projections from the (011) and $(01\bar{1})$ crystallographic axes are exhibited. The optimized structure is shown in the bottom of Fig. 3-5. Although the adsorbed O_2 molecule is stable, the molecule again dissociates when we extend the boundary condition of the unit cell from the 2×1 to the 2×2. (See Fig. 3-6.) Two arrows in Fig. 3-6 mean the calculated forces 0.08Ry/a.u. on the two O atoms. The charge contour map of the $(01\bar{1})$ plane shown in Fig. 3-6 again exhibits the electron transfer from the Si dimer into the antibonding π orbitals of the O_2 molecule. In these geometries of Figs. 3-5 and 6, the compositions of the O atoms per

surface Si atom are different. We have compared the stability in Fig. 3-5 with that in Fig. 3-6. In general the comparison of the stabilities should be done under the condition of the same stoichiometry. At first we have summed up the total energy per 2×1 unit cell of the geometry of the bottom of Fig. 3-5 and that of the clean Si(100) reconstructed surface and then we have compared the sum with the total energy per 2×2 unit cell of the geometry in Fig. 3-6. These two total energies correspond to those of the following two systems, respectively: (1)The O_2 molecules aggregate and make a domain of the 1ML coverage preserving the half of the Si(100) surface clean. (2)The O_2 molecules are scattered on the Si(100) surface uniformly and the resulting coverage is 0.5ML. The calculated total energy of the system(1) is $0.28eV$ higher than the that of the system(2). If we optimize the geometry in Fig. 3-6, the amount of the difference of two total energies is increased. So that we have concluded that when the O_2 molecule approaches the site B the molecular adsorption of oxygen is unfavorable rather than the dissociative adsorption. On each site of A and B, the O_2 molecule dissociates and each O atom is forced toward the dimer.

On each site of C and D, between the dimers rows, the O_2 molecule moves to lie on the surface with its axis tilted to the dimer bond axis and then it dissociates. The series of the pictures in Fig. 3-7 shows the sequence of the geometry optimization on the site C. When we place the molecule on the site D, the resulting pictures of the sequence of the geometry optimization is similar to that on the site C. (We do not show it here.) Each O atom is forced to sit on the center site between the top and second layer Si atoms after the dissociation of the O_2 molecule. (See the bottom of Fig. 3-7.) The surface Si dimer is twisted and buckled. Although we do not show the contour map of the charge density here, we would like to say that the electron transfer again occurs and causes dissociation of the O_2 molecule.

The spin state of the molecular oxygen is triplet[52] which can be reproduced in our present calculation. (See section 2.2) We have therefore checked the effect of the spin on the O_2 molecules on these four sites A$\sim$D by performing the calculation in the local spin density approximation with use of the same pseudopotentials and the same basis set as shown in

chapter 2. Then we have confirmed that, on each site of A∼D, as O_2 molecule approaches to the surface from a distance the spin state varies from triplet and then to doublet and finally to the singlet state during the geometry optimization. Then the molecule again dissociates. The spin polarized state of oxygen molecule disappears after the electron transfer from the dangling bonds of the Si dimer into the antibonding π orbitals of the O_2 molecule. This can be easily understood by the schematic diagram (See Fig. 3-8.) which shows the electron configurations of the O_2 molecule before and after the electron transfer.

In conclusion of this section, we have found that oxygen dissociates on almost all sites of the reconstructed Si(100) surface. During the optimization the calculated total energies decrease monotonically on all sites of the four A∼D. Since these sites cover almost all possibilities of the adsorption of the molecular oxygen we have concluded that there are no (meta)stable states for molecular oxygen on the Si(100) surface. The mechanism of dissociation of molecular oxygen is generally understood as the electron transfer from the dangling bonds of the Si dimer to the antibonding π orbitals of the O_2 molecule. If we extend the size of the unit cell, i.e. the thickness of the slab or the size of the lateral periodic boundaries, the interfearance of the neighboring O_2 molecules decreases. The dissociative adsorption of the oxygen therefore occurs more easily. The molecular adsorption of the oxygen would be realized only in the case of the sudden covering of the Si(100) surface by 1ML O_2 molecules as is shown in Fig. 3-5 if some experimental techniques permitted.

3.2 Adsorption of an O atom on the Si(100) surface

After the dissociation of the O_2 molecule each O atom is adsorbed on the Si(100) surface. To obtain the final stable structures of the adsorbed O atoms, we have fully optimized the atomic configurations of the O atom and the surface Si atoms according to the calculated forces. At the first step of the optimization we have adopted the 4 layers Si slab and the vacuum corresponding to 4 layers. The vacuum region has been reduced since we do not need

to place an O atom far from the surface in this stage. Then we have confirmed that the optimized geometries are still stable when the thickness of the Si slab is extended to 8 layers. The 2 × 1 lateral periodic boundary condition and the C_2 symmetry are again imposed during the optimization. We have placed O atoms on equivalent sites on both sides of the slab. We have found there are three adsorption sites for the adsorbed O atom depending on which site the preceding molecule dissociates.

When the molecule dissociates on the site A or B, the resulting adsorption site of the O atom is just on the dimer. (See Fig. 3-9.) Again the site A is just on the dimer and the site B is between the two neighboring dimers as shown in Fig. 3-3 in the previous section. The O atom and the surface Si atoms are located on the same (011) plane. The bond length and angle of the Si–O–Si complex are 1.9Å and 74°, respectively. The atomic configuration is stable against the displacement of the O atom away from the (011) plane. (See the directions of the calculated forces in the top view of the upper panel of the Fig. 3-9.) The difference of the total energies of the clean and oxygen adsorbed surfaces corresponds to the heat of formation. The heat of formation dE of the oxygen adsorption is defined by an equation

$$E_{O_2} + E_{Si_{surf}} = E_{2O+Si_{surf}} + 2dE \quad .$$

In the equation, the E_{O_2} and the $E_{Si_{surf}}$ mean the total energies of the oxygen molecule and the clean Si(100) surface, respectively. The $E_{2O+Si_{surf}}$ means the total energy of the oxygen adsorbed silicon surface. The resulting value of the dE is $2.1eV$,namely, the adsorption of the O atom on the site of Fig. 3-9 is exothermic.

When the O atom moves from the position toward the dimer bond and then intervenes the two Si atoms of the dimer, the most stable geometry is achieved. (See Fig. 3-10(a).) Again this geometry is stable against the displacement of the O atom. (See upper panel in Fig. 3-10(a).) The bond length and angle are $1.7\mathring{A}$ and 174°, respectively. The heat of formation dE is 3.1eV. The charge contour map in the (011) plane is shown in Fig. 3-10(b). The charge density indicates the ionic feature of the Si–O–Si bonds. The electron transfer occurs from the

dangling bonds of the surface Si atoms to the O atom. The dimer structure disappears at this stage. The fact is consistent with the disappearance of the 2×1 pattern of the low energy electron diffraction (LEED) of the Si(100) surface upon the oxidation below 1ML oxygen coverage. (See for example reference [38].)

When the O_2 molecule dissociates on site C or D (Again C and D are between the dimers rows as shown in Fig. 3-3 in previous section), each O atom of the molecule is forced to sit on the site between the top and second layer Si atoms. As for an O atom on the site C or D, we have started the geometry optimization from its initial position between the top and the second layer Si atoms. In this case, the O atom is forced away from the (011) plane of the Si dimer and finally sits on the site shown in Fig. 3-11 which shows the projections of the top and side views. The bond length between the O atom and the nearest Si atom is $1.9\mathring{A}$. The bond angle of the Si–O–Si complex consisting of the top and second layer Si atoms is $46.4°$. The surface dimer is tilted and buckled upon the oxygen adsorption. The lower Si atom of the dimer is away from the (011) plane. The corresponding heat of formation dE is 1.7eV.

We have compared the Mulliken charge of the O atom in one of the three (meta)stable configurations with the others. The Mulliken charge of the atom τ is expressed as

$$\sum_{\alpha,\beta,n,k}^{occup} C_{\alpha}^{nk*} S_{\alpha\beta}^{k} C_{\beta}^{nk} \quad ,$$

where the suffix α means the gaussian basis on the site τ and the β means the whole gaussian basis. The C_{α}^{nk} and the $S_{\alpha\beta}^{k}$ mean the eigenvectors of the wave function ψ_{nk} and the overlap matrices shown in the chapter 2, respectively. In this thesis we use the pseudopotentials so that the calculated Mulliken charge is that of the valence electrons. The number of the transferred electrons on an atom is therefore obtained by subtracting the number of its valence electron from its Mulliken charge. The numbers of the transferred electrons to the O atoms in the two metastable geometries in Figs. 3-9 and 11 are 0.6 and 0.7, respectively. On the other hand, in the most stable geometry of Fig. 3-10 the O atom obtains 1.2 electrons. The ordering of the magnitude of the transferred electrons in the three geometries does not correspond to that of

the heat of formation. However, one can notice that in the most stable geometry of Fig. 3-10 the O atom gets numerous electrons than other O atoms. According to the Mulliken charge analysis of the most stable configuration of Fig. 3-10, the neighboring two Si atoms lose 0.6 electrons per atom.

In conclusion, there ate three (meta)stable adsorption sites for atomic oxygen on the Si(100) reconstructed surface. Each adsorption site of the O atom depends on which site the preceding molecule dissociates. The most stable site is between the two Si atoms of the surface dimer in Fig. 3-10, which is achieved after (1)the dissociation of the molecular oxygen on the dimers row, site A or B, and (2)the diffusion of the O atom into the dimer bond. In the most stable geometry, the Si–O bond has an ionic feature. (See the contour map in Fig 3-10(b).) The O atom obtains 1.2 electrons from the neighboring two Si atoms. In the three (meta)stable configurations of our present calculation, the bond length between the Si atom and O atom varies from $1.6\mathring{A}$ to $1.9\mathring{A}$. This range of the bond length is still invariant when other oxygen comes and then makes the new Si–O bonds, which will be shown in section 3.4. The resulting Si–O lengths, Si–O–Si angles, heats of formation dE, and the numbers of the transferred electrons on the O atoms δ^- in the three (meta)stable configurations are summarized in table 3.1.

Table 3.1: Calculated results for the three (meta)stable geometries

geometry	Si–O	∠Si–O–Si	dE	δ^-
Fig. 3.9	$1.9\mathring{A}$	74°	$2.1eV$	0.6
Fig. 3.10	$1.7\mathring{A}$	174°	$3.1eV$	1.2
Fig. 3.11	$1.9\mathring{A}$	46°	$1.7eV$	0.7

3.3 Comparison with the experimental results

By performing the first principles calculations, we have now obtained the microscopic picture of the oxygen adsorption on the Si(100) surface. The results are free from any empirical

parameters which are constructed to fit with the experimental results. It is very important to investigate whether the theoretical results can explain the experimental results or not.

We have calculated the vibrational energies and the valence Density of States (DOS) for adsorbed oxygen atoms in the three (meta)stable geometries shown in Figs. 3-9$\sim$11. The results have been compared with the experimental data available, i.e. the High Resolution Electron Energy Loss Spectroscopy (HREELS)[16] and the UPS[18] of the oxygen adsorbed Si(100) surfaces.

According to the data of the HREELS[16], the vibrational energy, which is assigned to the surface normal mode of an adsorbed O atom, scatters from 91meV to 98meV with changing oxygen coverage. We have calculated the vibrational energies of the adsorbed O atoms in the geometries of Figs. 3-9 and 10 in which the shapes of the Si–O–Si complexes are symmetric and easy to estimate the vibrational energies. We have moved the three atoms of the Si–O–Si complexes in the surface normal directions as those of a free molecule as is shown in Fig. 3-12, i.e. symmetric stretching mode. Since the mass of the O atom is much smaller than that of the Si atom, the motions of the two Si atoms are not noticeable. For each geometry of Figs. 3-9 and 10, we have calculated the total energies of four atomic configurations around the stable position. The total energies have been interpolated as the parabolic functions of the displacements of the O atoms, and then the vibrational energies have been obtained as those of the harmonic oscillators. The calculated vibrational energies in Figs. 3-9 and 10 are 81meV and 80meV, respectively. The results show agreements with the experimental values within a reasonable error of the local density approximation. In general, the vibrational energies of the localized modes are determined by the local bond configurations and the corresponding force constants.[36] The bond angle of the Si–O–Si complex in Fig. 3-9 is smaller than that in Fig. 3-10. If the force constants of the Si–O bonds in these two geometries were equal, the vibrational energy of the O atom in Fig. 3-9 would be larger than that in Fig. 3-10. However, in the geometry of Fig. 3-10 the force constant of the Si–O bond is larger than that in Fig. 3-9 so that the resulting vibrational energies in Figs. 3-9 and 10 happen to fall into the same

value. This result is an example of what Ibach et al.[7] pointed out. It is dangerous to treat the local vibrational energies as the fingerprints of the local atomic configurations. It is therefore impossible to select one of the two configurations in Figs. 3-9 and 10 only from the comparison of our results with the data of the experiment. In conclusion, both of these geometries are candidates of the structures which are realized under the experimental condition of the HREELS.[16]

The UPS measurement[18] shows the appearance of three new peaks upon the 1.5 monolayer (ML) oxygen adsorption and the successive sample annealing at 700°C. The separations among the peaks are 3.3eV between the first and the second peaks (in increasing energy level) and 3.1eV between the second and the third, respectively. The results are shown in Fig. 3-13. The arrows in the figure denote the surface state of the Si(100) surface which disappears after the oxygen adsorption. We have compared the calculated Density of States (DOS) in the three (meta)stable geometries in Figs. 3-9$\sim$11 with the UPS data. The calculated DOS are shown in Figs. 3-14(a)$\sim$(c) with corresponding geometries on the right hand side in the order of the increasing binding energy of the adsorbed oxygen atom. The DOS of the clean surface of the symmetric dimer model in Fig. 3-1 is also shown in the Fig. 3-14(d) for comparison. Although the oxygen coverage in these geometries 0.5ML dose not correspond to the experimental value 1.5ML, the calculated DOS of the Fig. 3-14(c) shows the appearance of three new peaks in the valence band region as in the experimental results. The three peaks are denoted by three arrows in Fig. 3-14(c). The separations among the peaks, 3.9eV between the first and second peaks (in increasing energy level) and 2.0eV between the second and third, show reasonable agreements with the UPS data. In other metastable geometries, the calculated DOS does not exhibit the prominent three peaks. These results indicates that the appearance of the three peaks does not depend on the oxygen coverage but depends on the atomic configuration of Si and O atoms.

The most stable geometry in Fig. 3-10 explains both of the two experimental results according to the comparison of our present results with the experiments. We have further clarified

the origin of three peaks in the DOS which characterizes the electronic structure of the Si–O bonds. The Local Density of States (LDOS) in the geometry of Fig. 3-10 has been calculated and compared with the corresponding DOS in Fig. 3-14(c). The LDOS of the gaussian base α is expressed as

$$D_\alpha(\varepsilon) = -Im \sum_{n,k,\beta}^{occup} \frac{C_\alpha^{nk*} S_{\alpha\beta}^k C_\beta^{nk}}{\varepsilon - \varepsilon_{nk} + i0^+} \quad , \tag{3.1}$$

where α and β are the indexes of the gaussian bases and C_α^{nk} is an element of the eigenvectors of the wave function $\psi_{n,k}(\mathrm{r})$. The $S_{\alpha\beta}^k$ means the overlap integral of the two elements of the gaussian bases set. (See the previous section 2.1.) The LDOS of an atomic orbital with the angular momentum l is expressed as

$$D_{l,\tau}(\varepsilon) = \sum_\alpha D_\alpha(\varepsilon) \quad . \tag{3.2}$$

The $\sum_\alpha$ means the summation over the gaussian basis of the same angular momentum l at the same atomic site τ. The LDOS of the orbitals localized on the surface Si and O atoms in Fig. 3-10 are shown in Figs. 3-15(a) and (b), respectively. In the calculation, the value of 0.03Ry (0.4ev) has been adopted as the 0^+ in equation (3.1). For the explicit expression of the wave function, we have defined the x and y directions as those normal and parallel to the bond direction of the Si–O–Si complex, respectively. The z direction has been fixed normal to the surface. The LDOS's of the other Si atoms of the slab, which are not shown here, are similar to that of the bulk silicon. By comparing Fig. 3-14(c) with Figs. 3-15(a) and (b), the lowest peak of the three is assigned to the LDOS of the O p_y orbital and the uppermost peak is assigned to that of the O p_x plus p_z orbitals. The middle peak can not be clearly expressed by the LDOS of the localized orbitals of the O or Si atom. It may have a hybridized character. Since the Si–O bond of the Si–O–Si complex in Fig. 3-10 is in the y direction, the bonding orbital of the O atom should be expressed by the O p_y component. On the other hands, the x and z are nonbonding directions. It is therefore reasonable that the O p_x and p_z nonbonding orbitals are constituting the states of higher energy level than the level of the O p_y bonding orbital. This electronic structure agrees with the interpretation of experimental work by Hollinger et al.[18]

They have guessed the electronic structure by comparing their results with the band structure calculation of the bulk SiO_2.[45] It is of interest to note that the electronic level structure which is similar to that of the bulk SiO_2 has already appeared in such an early stage of the oxidation.

3.4 Penetration and adsorption of oxygen through oxygen covered surface

For the most stable geometry in Fig. 3-10, we have found that another O atom makes the Si–O–Si chain in the $(01\bar{1})$ direction and constitutes a stable atomic geometry when it approaches the remaining hollow bridge site. (See Fig. 3-16 which shows the side views from the (011) and the $(01\bar{1})$ directions in addition to the top view.) The resulting heat of formation dE is 2.8eV. This geometry corresponds to 1 monolayer (1ML) oxygen coverage. The surface Si atoms go back close to the ideal positions of the bulk and the oxygen atoms are located at heights $0.11\mathring{A}$ above the surface Si atoms. (Batra et al.[14] have obtained the same adsorption site of the O atom by the cluster calculation and the resulting configuration is quantitatively different with our result.) In this case, all Si dangling bonds on the surface are terminated by the adsorbed O atoms. It seems that the electron transfer into the antibonding π orbitals of the additional molecule can not occur. It is of interest to ask how does oxidation continue on the 1ML oxidized surface.

According to our present calculation the O atoms usually sit on the sites with two neighboring Si atoms. (In the following we call this site as "bond center site".) The bond center sites between the top and second layer Si atoms in Fig. 3-16 are therefore the candidates of the new adsorption sites of the oxygen atoms. In the calculation, the 2 × 1 unit cell of the 1ML oxygen covered surface is adopted again. The unit cell is perpendicular to the previous 2 × 1 unit cell. The longer axis of the 2 × 1 unit cell is in the (011) direction and shorter axis is in the $(01\bar{1})$ direction. We have adopted the C_{2v} symmetry which keeps the geometry invariant for the 180° rotation around surface normal axis and mirror operations with respect to the (011) and $(01\bar{1})$ planes. The equivalent geometries on both sides of the slab have been again imposed. We have

performed the geometry optimization with the additional O_2 molecules on both sides of the slab. The O_2 molecules are placed parallel to the surface and perpendicular to the Si–O–Si chains in the vicinity of the bond center sites. When we place each O_2 molecule without any relaxation of other atoms in Fig. 3-16, the force on each O atom of the molecules acts to remove the atom from the surface. When the Si and O atoms on the Si(100) surface are relaxed in the (011) direction and make a space between the neighboring chains of the Si–O–Si bridge bonds, the new O_2 molecules can dissociate and each atom sits on the bond center site. (See Fig. 3-17 which shows one of the two equivalent sides of the slab.) The resulting atomic configuration of newly adsorbed O atom and the two neighboring Si atoms is similar to the stable site of the O atom in the bulk silicon.[20] The displacement of the top layer Si atom is $0.7\mathring{A}$ in lateral direction and $0.5\mathring{A}$ upward in normal direction. The second layer Si atom which is not the neighbor of the O atom moves $0.2\mathring{A}$ downward. (See near the edges in Fig. 3-17.) The bond length and bond angle of the newly formed Si–O–Si complex are 1.6Å and 148°, respectively. The values are close to those of the α–quartz. On the other hand the bond angle of the newly formed O–Si–O complex consisting of the second layer Si atom is 81° which is close to that of the stishovite. It is well known that the phase of the stishovite appears under the hydrostatic pressure more than 10GPa at the room temperature.[46] It is therefore a surprising fact that the structure which is similar to the high pressure phase has already appeared in an initial stage of the oxidation. Although the large strain of surface Si atoms in this case is unfavorable to the oxygen adsorption, this reaction is still exothermic. We have calculated the heat of formation dE which is now redefined as

$$E_{O_2} + E_{1ML\ O\text{–}Si_{surf}} = E_{2O+1ML\ O\text{–}Si_{surf}} + 2dE \quad ,$$

where $E_{1ML\ O\text{–}Si_{surf}}$ means the total energy of the 1ML oxygen covered Si(100) surface. The resulting heat of formation dE is 1.2eV per new O atom. The charge contour map in Fig. 3-17 shows that the new Si–O bonds are ionic again. Although the new oxygen can not get electrons from the surface dangling bonds, which do not exist now, it gets electrons from both of the top

and second layer Si atoms. According to the Mulliken analysis, the newly adsorbed O atom gets 1.2 electrons. The number of transferred electrons is identical to that of the adsorbed O atom in Fig. 3-10. However, in the case of Fig. 3-17 the O atoms are placed close to each other and the electrostatic potential between the charged O atoms may cause the increase of the total energy of the system and then the resulting heat of formation $1.2eV$ is decreased smaller than the value $3.1eV$ of Fig. 3-10.

In the geometry of Fig. 3-17, the remaining Si–Si bonds between the top and the second layer Si atoms are stretched, shown in the edges of the figure. These are candidates of further adsorption sites of O atoms. We have placed another O atom on the site. The geometry optimization has been performed again and now the 1 × 1 periodic boundary condition has been adopted. We have adopted the C_2 symmetry which keeps the structure invariant for the 180° rotation around the surface normal axis. According to the geometry optimization we have obtained the stable geometry shown in Fig. 3-18. In Fig. 3-18, the sequential numbers are assigned to the top and second layer Si and O atoms for the detailed explanation of the geometry. The same numbers are assigned to the equivalent atoms of the periodic boundary and the C_2 symmetry. The top layer $Si^{[1]}$ and $O^{[3]}$ atoms are lifted up from their positions in Fig. 3-17 by $0.78\mathring{A}$ and $1.31\mathring{A}$, respectively. The volume of the region of the top and second Si layer has been expanded 83% from the value of the bulk. The bond length of the $Si^{[1]}$–$O^{[3]}$ is stretched to $2.00\mathring{A}$ and the angle of the $Si^{[1]}$–$O^{[3]}$–$Si^{[1]}$ complex is 147.9°. These values are larger than those of the α–quartz. Next, let us review the local structure of the newly adsorbed $O^{[4]}$ atoms connecting the top and second layer $Si^{[1,2]}$ atoms. The newly adsorbed $O^{[4]}$ atoms are located away from the $(01\bar{1})$ plane. (See top view of Fig. 3-18.) The $Si^{[1,2]}$–$O^{[4]}$ bond length and the angle of the $Si^{[1]}$–$O^{[4]}$–$Si^{[2]}$ complex are $1.7\mathring{A}$ and 130.1°, respectively. The bond angle of the $O^{[4]}$–$Si^{[1]}$–$O^{[4]}$ complex is 87.3°. These values of the local structure are again close to those of the stishovite. We have therefore concluded that the system is compressed in lateral directions at the local region just below the surface. The resulting heat of formation is 1.5eV per $O^{[4]}$ atom. At this stage the oxygen adsorption is still exothermic surprisingly. If we were

able to remove any periodic boundary condition in the calculation, the system would show a volume expansion in both of lateral and vertical directions.

In conclusion of this section, the local structures which are similar to that of the α–quartz and stishovite appear after the penetration of the O atoms through the 1ML oxidized surface. The resulting local structures are summarized in table 3.2, in which O^{new} means the newly adsorbed O atom in Fig. 3-17. However, in these geometries of Figs. 3-17 and 16 the coordination numbers of the oxygen atom around the Si atoms do not completely correspond to four, i.e. the value of the SiO_2. In the geometry of Fig. 3-17, the top Si atom is surrounded by three O atoms and the next layer Si atom is surrounded by two O atoms. On the other hand in the geometry of Fig. 3-18, the top Si atom is surrounded by four O atoms and the next layer Si atom is surrounded by two O atoms. We expect the similar situation occurs in the conditions of the experiments[18, 25] which show the chemical shifts of the Si $2p$ core levels because of the different coordination numbers of the O atoms around the Si atoms.

Table 3.2: Calculated results for the oxygen penetration

geometry	configuration	length or angle	similar structure
Fig. 3.15	O^{new}–Si	$1.6\mathring{A}$	α–quartz
	$\angle$ Si–O^{new}–Si	148°	
	$\angle$ O^{new}–Si–O^{new}	81°	stishovite
Fig. 3.16	$Si^{[1,2]}$–$O^{[4]}$	$1.7\mathring{A}$	stishovite
	$\angle$ $Si^{[1]}$–$O^{[4]}$–$Si^{[2]}$	130°	
	$\angle$ $O^{[4]}$–$Si^{[1]}$–$O^{[4]}$	87.3°	

Chapter 4

Discussion

We have found that the oxygen molecule dissociates at almost all sites of the Si(100) surface and then the O atoms are adsorbed on three (meta)stable sites preserving or decomposing the Si dimer. The adsorption site depends on which site the preceding molecule dissociates. We have further found that the oxygen can penetrate through the 1ML oxidized Si(100) surface and each O atom is absorbed on the bond center site between the first and second layer Si atoms. That causes peculiar distortions of the Si atoms and the volume expansion of the substrate. The local structures of the formed Si–O–Si complexes are similar to those of the two phases of the SiO_2, i.e. the α–quartz and the stishovite. Although the oxidized film may be compressed, the oxygen reaction is still exothermic.

These results give us the general informations about the silicon oxidation. In this chapter, we discuss possible configurations of oxygen on the silicon surfaces and the kinetics of the oxidation. Finally we discuss what kind of the theoretical works will be useful for further understanding of the oxidation.

4.1 The possible geometries of adsorbed oxygen

4.1.1 O_2 molecules on silicon surfaces

The possibilities of the molecular adsorption of the oxygen on the Si(100) surface have been proposed by theoretical works[10, 15] with use of the molecular orbital methods for clusters.

However, we have to point out that the possibilities of the adsorption of the O_2 molecule on the silicon surfaces should be carefully investigated by calculating the forces. First of all, the atomic configuration of the O_2 molecule, i.e. the O-O bond length and its tilt angle, should be fully optimized according to the calculated forces. Next, when the calculated forces are reduced enough one has to confirm that each atom is forced to go back when it moves away from its optimized position in any direction. These theoretical works[10, 15] have not been done in such a manner. On the other hand, we have shown the dissociation of the O_2 molecule at almost all sites on the Si(100) surface in section 3.1. Thus it is hard for us to agree with these theoretical works.[10, 15]

The study of the electronic structure of O_2 molecules on the surface reveals an interesting aspects: The doublet spin states can be a good evidence of the adsorption of the O_2 molecules on Si surfaces. Although O_2 molecules have been shown to be unstable on Si(100), the following argument may be useful to find a possible molecular adsorption on other surfaces of Si. Let us review the schematic diagram of the electronic configurations of the O_2 molecule. (See Fig. 3-8.) The dissociation of the O_2 molecule occurs after the perfect occupation of the antibonding π orbitals by two electrons which transfer from the surface Si atoms. Then the resulting spin state is singlet. On the other hand, when the molecule can obtain only one electron, one of the two antibonding π orbitals is the fully occupied state and the other is remained to be the half occupied state and then the resulting spin state is doublet. In this case the oxygen molecule exists on the silicon surface with its doublet spin state. When the molecule lies on the surface, both of the two O atoms are close to the surface and then the molecule obtains two electrons and dissociates. Thus we can not agree with the model of the Höfer et al.[20] who have proposed the model of the lying O_2 molecule on the Si(111) surface. When the O_2 molecule stands on the surface with arbitrary tilted angle, one of the two O atoms of the molecule is connected to the surface. The molecule therefore can obtain only one electron which is insufficient for the dissociation. What we want to stress here again is that the spin polarized state is a clear evidence of the adsorption of the O_2 molecule. The doublet spin states

of the adsorbed O_2 molecules may be able to be observed by several experimental techniques, for example the spin polarized photoemission spectroscopies, etc. Recently the paramagnetic spin states have been found on the oxidized Si(111) surface.[47] Although this result includes several uncertainties, this may mean the existence of the spin polarized O_2 molecules on the surface.

4.1.2 O atoms on silicon surfaces

As for the adsorption of the atomic oxygen on the Si(100) surface, we would like to propose the realization of the adsorption on metastable sites. We have found the two metastable sites of the adsorbed O atom (See Figs. 3-9, and 11.) in addition to the most stable site in Fig. 3-10. We have performed the comparison of our results with the experimental data. The calculated values in the most stable geometry show good agreements with the results of both HREELS[16] and UPS[18]. On the other hand the values in the other two metastable geometries do not completely agree with those of these experiments. This result may indicate that, although the most stable geometry is abundant in typical experimental conditions, the other two metastable geometries which preserve the dimer structure should be realized only under well-controlled experimental conditions, i.e. low oxygen coverages or low temperatures of the samples or other non-equilibrium conditions. The metastable O atoms may play an important role to determine the atomic structure of the oxide films. In this subsection we discuss the possibility of the metastable configurations of the adsorbed O atoms like in Figs. 3-9 and 11 which may have been missed in the previous experiments.

The vibrational energy of the O atom on the metastable site of Fig. 3-9 is identical to that on the most stable site shown in Fig. 3-10. The calculated values reasonably agree with the data of the HREELS[16], so one cannot eliminate the possibility of the geometry in Fig. 3-9. The geometry shown in Fig. 3-9, as well as the geometry in Fig. 3-10, is a candidate of the adsorption site for the O atom in the experimental condition[16]. Meanwhile there is another indirect evidence of the metastable site of the adsorbed O atoms on the Si(100) surface. Yang

et al.[37] performed the experiment of the Low Energy Electron Diffraction (LEED) of the Si(100) surface and obtained a 2 × 1 diffraction pattern. They have proposed the buckled and twisted configurations of the Si dimer on the Si(100) surface by analyzing the LEED pattern. Although, the twisted dimer model of the Si(100)2 × 1 surface disagrees with other experimental and theoretical works[43, 44], it agrees with our present result which shows the twisted structure of the surface Si dimer. (See Fig. 3-11.) We would like to point here the possibility of the existence of the O atoms on the surface in the experimental condition by Yang et al.[37] If so the Si dimer should be twisted by the O atom on the metastable site like Fig. 3-11.

Unfortunately, the features of the calculated DOS of these two metastable structures in Figs. 3-9, and 11 do not exhibit noticeable differences from that of the clean Si(100) surface. So that it is hard to identify these metastable geometries by UPS or any other spectroscopy. However, we believe that careful experiments or other new techniques will be able to show the metastable sites of the O atoms on the Si(100) surface in which the adsorbed O atoms preserve the dimer structure of the Si(100) surface. Recently the preservation of the 2 × 1 periods of the surface structure at the interface between SiO_2 and Si(100) substrate has been found by grazing incidence X-ray diffraction method.[48] The sample was fabricated by molecular beam deposition, i.e. silicon deposition in an O_2 atmosphere on silicon wafers, which may provide the condition of the non-equilibrium. We expect that the O atoms on metastable sites play an important role in the oxidation under certain non–equilibrium conditions.

4.2 The kinetics of oxidation on the Si(100) surface

4.2.1 The two stages of oxidation

It is said that there are two different stages in oxidation on the Si(100), (111) or other surfaces, i.e. the fast oxidation stage in which the coverage quickly achieves 1ML and the slow oxidation stage in which the film of silicon oxide appears.[40] The kinetics is usually understood by the existence of two adsorption states of oxygen on the surface: one is the molecular state and

the other is dissociative state. But our present calculation shows that there are no metastable sites of the O_2 molecule on the Si(100) surface. We have found that the oxygen dissociates at almost all sites on the Si(100) surface and the O atoms adsorb on three (meta)stable sites on the surface preserving or decomposing the surface Si dimer. Finally the additional molecules penetrate through 1ML oxidized surface and then dissociates. From our calculation the two stages of the oxidation on the Si(100) surfaces can be explained as follows: First, the dissociative oxygen adsorption on the surface occurs. Second, the oxygen molecule penetrates through the surface with the aid of the thermal motions of the surface atoms. The last picture is consistent with the result that the rate of the oxide film formation is increased as temperature raises.[40]

4.2.2 The probability of oxygen adsorption on the Si(100) surface

Now we have to comment on some experimental results of the probability of the oxygen adsorption on the Si(100) surface within the range of 1ML oxygen coverage. Experimental works of molecular beam scattering[39] have been done and then the sticking probability of incident O_2 molecule has been estimated. The value is very low at any surface temperature, of the order of 1/1000. This means that almost all oxygen molecules are not adsorbed on the Si(100) surfaces but scattered from the surface. In addition to that, an increase of the probability of the initial oxygen adsorption by alkali metal adsorption on silicon surface has been reported by the Auger electron spectroscopy.[49] The adsorbed alkali metals have been expected to raise up the Fermi level relatively above the energy level of the antibonding π orbital of the molecular oxygen causing the charge transfer in the π orbital of the O_2 molecule and resulting in dissociation and adsorption of the oxygen. (This explanation comes from the theoretical results of the dissociation of the CO molecule on Ni surfaces assisted by the adsorption of the alkali metals.[50]) On the other hands, our present result says that oxygen can dissociate at any site on the Si(100) surface. We have found no potential barriers during the dissociation of the molecule. The electron transfer from surface dangling bonds into molecular antibonding

π orbitals occurs without any assistance. Our result therefore seems to be inconsistent with the experimental results.[39, 49] However, we have to keep in mind that each O_2 molecule has its intrinsic motions, i.e. translation, rotation, and vibration. In our calculation the intrinsic motions of the O_2 molecules are not taken into account. During the geometry optimization the trajectory of the molecule does not correspond to the trajectory of the motion of the oxygen on the surface. In fact the adsorption of the molecule occurs when it is trapped by a valley of the adiabatic surface during the motion. Otherwise the molecule is scattered from the surface. Whether the oxygen is adsorbed or scattered depends on the initial conditions of the motion of the incident O_2 molecule. It is therefore impossible to compare our results directly to these experimental results. One, who wants to theoretically estimate the sticking probability of the O_2 molecule, has to perform the molecular dynamics (MD) and has to deal with the calculated results statistically. Unfortunately it is impossible to perform the MD without any efficient model of the interactions among the Si and O atoms[51] because of the limited potentials of the computers. Furthermore, the MD simulation for oxygen reactions on the silicon surfaces needs the consideration of the electron transfer from the surfaces to O atoms. At present, nobody knows how to do it.

4.2.3 The formation of the oxide film

Finally let us discuss the mechanisms of the oxide film formation. The oxide has the Si–O–Si local structures in it. According to the present calculation, the binding energy of the O atom is at least larger than 6eV per Si–O–Si complex. On the other hands, when an O_2 molecule is in the oxide film it can obtain no electrons from the oxidized area. The molecule can diffuse in the oxidized area without dissociation and adsorption since the dissociation of it is derived by the electron transfer into its antibonding π orbitals. We therefore expect that the O_2 molecule be able to diffuse with a lower activation energy than that of the O atom. If so the O_2 molecule can enter the non–oxidized area and then the new Si–O–Si complex is formed after the dissociation of the molecule. According to this picture the flat interface between oxide and silicon surface[1]

can be understood as the result of the layer by layer oxidation. This model corresponds to what we have demonstrated in this thesis. Indeed we have put oxygen atoms or molecules on the Si(100) reconstructed surface layer by layer, i.e. we have put a layer of oxygen molecules or atoms on the surface and then we have put an additional layer of O_2 molecules on the 1ML oxygen covered surface. Finally what we have found is that the structures which are similar to the high pressure phase of the SiO_2 appear after the oxidation. The result indicates that the system is compressed in lateral directions which may cause some kinds of the damages of the silicon substrates, i.e. vacancies, interstitial atoms, dislocations, and stacking faults, etc. The pressure in the lateral directions may lead to the appearance of new phases in the oxide film or in the silicon substrate, which cannot be realized under the hydrostatic pressure. The work of the TEM[1] which shows the new atomic configuration at the SiO_2/Si(100) interface suggests the existence of the new atomic structure of the SiO_2 or the silicon crystal.

4.3 For the further understanding of the oxidation

In this thesis we have obtained a microscopic picture of the oxidation. The theoretical success has been produced due to the localized basis set which enables us to express the compact valence wave functions of the O atoms efficiently. If we used the plane wave basis set, the huge number of the plane waves would be required for a well converged calculations. What is generally seen about of the adsorbed oxygen atom is that the O atom always sits between two Si atoms whether it comes on the surface or penetrates through the surface. The most stable site for the O atom is similar to the stable site of it in the bulk silicon[27], i.e. the bond center sites. The Si–O–Si complexes are formed in any stage of the oxidation. In the initial stage, the bond length and angle of the Si–O–Si complex are close to those of the α–quartz. When the oxidation proceeds, the values of the local lattice parameters become to be close to those of the stishovite. The Si atoms of the substrate show peculiar distortion and finally the volume of the substrate expands. We have proposed that at this stage the oxide part is compressed

in the lateral directions by deducing from the fact that the resulting atomic configurations are similar to that of the stishovite which is the high pressure phase of the SiO_2. We have thus obtained the microscopic picture of initial oxidation on the Si(100) surface. However, we have not answered the following questions which will become important problems in future when we try to make the further theoretical approach to silicon oxidation.

1. **Does oxygen aggregate on the silicon surfaces or at the interfaces between the oxide and silicon substrate ?**

2. **If it occurs, what is the most favorable stoichiometry of the oxygen on the surfaces or at the interfaces ?**

3. **How much do the stress and pressure arise at the interface and how do they affect the structure of the oxide film and the silicon substrate ?**

In this section we would like to propose what kinds of the theoretical works will be useful to answer these questions.

To answer the first and second questions, we must compare the total energy of the system with that of the different stoichiometry of the O and Si atoms since the effect of the entropies in solids may be negligible.[41] What is important at that time is to know the chemical potentials of the O and Si atoms. In general, the values of the chemical potentials of atoms in compounds can not be determined uniquely.[41] In this case we can know only the upper and lower limits of the chemical potentials of the Si and O atoms. The chemical potential of the O and Si atom on the Si surface or at the interface between the oxide and Si is determined as a difference of the total energies before and after relocating the atom. The value of the chemical potential varies depending on where the atom goes: into the silicon substrate, into oxide film, or into the vacuum. To obtain the well converged value of the chemical potential, the calculations of the total energies of the large enough unit cells are required.

To answer the last question, we have to perform the *ab-initio* calculation of the stress tensor with the same manner of the reference [42]. The stress tensor are obtained as the gradients of

the total energy with respect to the strain tensor. (The size and shape of the periodic boundary is now modified.) As we said in the introduction there is a large lattice mismatch between the silicon oxide and silicon crystal. The lattice mismatch causes the inhomogeneous stress at the interface between the oxide and silicon substrate. With use of the method of reference [42], we can perform the geometry optimization of atomic configuration under the inhomogeneous external stress tensor which is a useful tool to understand the atomic structure of the system. There is a possibility to discover new material phases of the oxide and silicon which are not obtained under the usual conditions of the hydrostatic pressures.

These theoretical approaches will be useful not only for the understanding of the silicon oxidation but for the general understanding of the formation of the films which have different structures from the substrates. We need a sufficiently large size of a unit cell when we perform a band-structure calculation. What troubles us in doing so is that the degree of freedom of the optimization is extraordinary increased. Indeed we have to optimize the stoichiometry of Si and O atoms and the shape and the volume of the unit cell in addition to the atomic coordinates. Rapid progress of the super computer will enable us to perform these works free from any empirical parameter.

Chapter 5

Concluding remarks

We have performed the *ab-initio* calculation of the total energy band structure and the force within the local density approximation for oxygen reactions on the Si(100) surfaces. The norm conserving nonlocal pseudopotentials and the gaussian basis sets have been used. For the calculation of the oxidized silicon surface, the repeating slab geometries have been used. The atomic configurations of the O atoms and the surface Si atoms are fully optimized according to the calculated forces toward the total energy minimized geometries. We have obtained the microscopic picture of the oxidation on the Si(100) surface, i.e. the dissociation of the O_2 molecule, adsorption of the atomic oxygen and then further oxidation of the surface accompanying the volume expansion of the substrate.

The phenomenon of oxidation is generally understood as follows

1. **The dissociation of the O_2 molecule occurs due to the electron transfer from the surface dangling bonds to molecular antibonding π orbitals.**

2. **The O atom is adsorbed between the two neighboring Si atoms and then it makes the Si–O–Si complex wherever it is adsorbed.**

3. **The electronic structure of the initially adsorbed O atom and Si atoms on the surface is surprisingly similar to that of the bulk SiO_2. The Si–O bonds show an ionic feature.**

4. **Further oxidation changes the local structure of the bond network of the Si and O atoms from that of the α–quartz to that of the stishovite. That means an increase of the pressure of the system.**

Although only the case of the oxidation on the Si(100) surface has been investigated, we expect that the resulting rules can be applied generally to the oxidation of other silicon surfaces. These results give us a fundamental knowledge about silicon oxidation and a basis for technologies of the silicon related electronic devices.

The present result has clarified for the first time the microscopic phenomenon of the oxidation by an *ab-initio* calculation. The band structure calculation for the oxidation on silicon surfaces with use of the plane wave basis set needs a huge number of the plane waves and corresponding large memories for the computation because of the compactness of the valence wave functions and because of the large volume of the unit cell. Meanwhile the band structure calculation with use of the localized basis set enables us to treat the atoms in the first row of the periodic table more easily. We have therefore chosen the gaussian basis sets for the wave function expansion.

Bibliography

[1] see for example, A. Ourmazd, D. W. Taylor, J.A. Rentschler and J. Bevk, Phys. Rev. Lett. **59**, 213 (1987);
A. Ourmazd, J.A. Rentschler, and J. Bevk, Appl. Phys. Lett. **53**, 743 (1988).

[2] H. Ibach, K. Horn, R. Dorn and H. Lüth, Surf. Sci. **38** , 433 (1973)

[3] H. Ibach and J.E. Rowe,Phys. Rev. b**9**, 1951 (1973); Phys. Rev. B**10**, 710 (1974).

[4] R. Ludeke and A. Koma, Phys. Rev. Lett. **34**, 1170 (1975).

[5] S. Fujisawa and M. Ogata and M. Nishijima, Solid State Commun. **21**, 895 (1977);
M. Nishijima, K. Edamoto, Y. Kubota, H. Kobayashi and M. Onchi, Surf. Sci. **158**, 422 (1985);
K. Edamoto, Y. Kubota, H, Kobayashi, M. Onchi and M. Nishijima J. Chem. Phys. **83**, 428 (1985)
A.J. Schell-Sorkin and J.E. Demuth, Surf. Sci. **157**, 273 (1985).

[6] J.H. Rechtien, U. Imke, K.J. Snowdon, P.H.F. Reijnen, P.J. Van den Hoek, A.W. Kleyn, and A. Namiki, Surf. Sci. **227**, 35 (1989).

[7] H. Ibach, H.D. Bruchmann, and H. Wagner, Appl. Phys. A**29**, 113 (1982).

[8] C.M. Garner, I. Lindau, C.Y. Su, P. Pianetta and W.E. Spicier, Phys. Rev. B**19**, 3944 (1979).

[9] H. Ibach, H.D. Bruchmann and W. Wagner, Appl. Phys. A**29**, 113 (1982).

[10] W.A. Goddard *III*, A. Redondo and T.G. McGill, Solid State Commun. **18**, 981 (1976).

[11] M. Chen, I.P. Batra and C.R. Brundle, J. Vac. Sci. Technol. **16**, 1216 (1979).

[12] S. Ciraci, S. Ellialtioglu and S. Erkoc, Phys. Rev. B**26**, 5716 (1982).

[13] N. Rosso. M. Toscano, V. Barone and F. Lelj, Phys. Lett. **113A**, 321 (1985);
V. Barone, F. Lelj, N. Rosso and M. Toscano, Surf. Sci. **162**, 230 (1985).

[14] I.P. Batra, P.S. Bagus and K. Hermann, Phys. Rev. Lett. **52**, 384 (1984); J. Vac. Sci. Technol A**2**, 1075 (1984).

[15] P.V. Smith and A. Wander, Surf. Sci. **219**, 77 (1989)
X.M. Zheng and P.V. Smith, Surf. Sci. **232**, 6 (1990).

[16] J.A. Schaefer, F. Stucki, D.J. Francel, W. Gopel and G.J. Lapeyre, J. Vac. Sci. Technol. **A1**, 640 (1983).

[17] C.Y. Su, P.R. Skeath, I. Lindau, and W.E. Spicer, J. Vac. Sci. Technol. **19**, 481 (1981).

[18] G. Hollinger and F.J. Himpsel, Phys. Rev. B**28**, 3651 (1983); J. Vac. Sci. Technol. **A1**, 640 (1983);
F.J. Himpsel, F.R. McFeely, A. Taleb-Ibrahimi, J.A. Yarmoff and G. Hollinger, Phys. Rev. B**38**, 6084 (1988).

[19] G. Hollinger J.E. Morar, F.J. Himpsel, G. Hughes and J.L. Jordan, Surf. Sci. **168**, 609 (1986).

[20] P. Morgen, U. Höfer, W. Wurth and E. Umbach, Phys. Rev. B. **39**, 3720 (1988);
U. Höfer, P. Morgen, W. Wurth and E. Umbach, Phys. Rev. B**40**, 1130 (1989).

[21] E.G. Keim, L. Wolterbeek, and A. van Silfhout, Surf. Sci. **180**, 565 (1987).

[22] J. Pollmann, P. Kruger, A. Mazur, and G. Wolfgarten, Surf. Sci. **152/153**, 977 (1985).

[23] H. Tokumoto, K. Miki, H. Murakami, H. Bando, M Ohno and K. Kajimura, J. Vac. Sci. Technol. A8, 255 (1990)
J.P. Pely and R.H. Koch, Phys. Rev. B**42**, 3761 (1990).

[24] F.M. Leibse, A. Amsavar, and T.-C. Chiang, Phys. Rev. B**38**, 5780 (1988).

[25] W. Ranke and Y.R. Xing, Surf. Sci. **157**, 353 (1985).

[26] A. Namiki, K. Tanimoto, T. Nakamura, N. Murayama and T. Suzaki, Surf. Sci. **203**, 129 (1988);
A. Namiki, K. Tanimoto, T. Nakamura, N. Ohtake and T. Suzaki, Surf. Sci. **222**, 530 (1989).

[27] M. Saito and A. Oshiyama, Phys. Rev. B**38**, 10711 (1988).

[28] A. Oshiyama, M. Saito, J. Phys. Soc. Jpn. **56**, 2104 (1987).

[29] P. Hohenberg and W. Kohn, Phys. Rev. **136**, B864 (1965);
W. Kohn and L.J. Sham, Phys. Rev. **140**, A1133 (1965).

[30] D. R. Hamann, M. Schlüter, and C. Chang, Phys. Rev. Lett. **43**, 1494 (1982);
G. B. Bachelet, D. R. Hamann, and M. Schlüter, Phys. Rev. **26**, 4199 (1982).

[31] J. Perdew and A. Zunger, Phys. Rev. B**23**, 5048 (1981).

[32] D.M. Ceperley and B.J. Alder, Phys. Rev. Lett. **45**,566 (1980).

[33] J.D. Levine, Surf. Sci. **34**, 90 (1973).

[34] The effect of the magic number of Si cluster is shown in, D. Tománek and M.A. Schlüter, Phys. Rev. Lett. **56**, 1055 (1986).

[35] M.T. Yin and M.L. Cohen, Phys. Rev. B**24**, 2303 (1981).

[36] See for an example, H. Ibach and D.L. Mills, *Electron Energy Loss Spectroscopy and Surface Vibrations* (Academic, New York, 1982).

[37] W.S. Yang, F. Jona, and P.M. Marcus, Solid State Comm. **43**, 847 (1982).

[38] L. Incoccia, A. Balerna, S. Cramm, C. Kunz, F. Senf and I. Storjohann, Surf. Sci. **189/190**, 453, (1987).

[39] J.R. Engstrom, and T. Engel, Phys. Rev. B**41**, 1038 (1990);
M.P. Dévelyn, M.M. Nelson, and T. Engel, Surf. Sci. **186**, 75 (1987).

[40] see for example, P. Gupta, C.H. Mak, P.A. Coon, and S.M. George, Phys. Rev. B**40**, 7739 (1989).

[41] Guo-Xin Qian, R.M. Martin and D.J. Chadi, Phys. Rev. B**38**, 7649 (1988);
J.E. Northrup, Phys. Rev. Lett. **62**, 2487 (1989).

[42] O.H. Nielsen and R.M. Martin, Phys. Rev. B**32**, 3780 (1985) , Phys. Rev. B**32**, 3792 (1985).

[43] N. Robert and R.J. Needs, Surf. Sci. **236**, 112 (1990);
Z. Zhu, N. Shima, and M. Tsukada, Phys. Rev. B**40**, 11868 (1989);
I. P. Batra, Phys. Rev. B**41**, 5048 (1989).

[44] R.M. Tromp, P.G. Smeenk, F.W. Saris, and D.J. Chadi, Surf. Sci. **133**, 137 (1983);
B.W. Holland, C.B. Duke, and A. Paton, Surf. Sci. **140**, L269 (1984),
R.J. Hamers, R.M. Tromp, and J.E. Demuth, Phys. Rev. B**34**, 5343 (1986).

[45] S.T. Pantelides and W. Harrison, Phys. Rev. B**13**, 2667 (1976).

[46] R.J. Hemley, A.P. Jephcoat, H.K. Mao, L.C. Ming, and M.H. Manghnani, Nature, **334**, 51 (1988).

[47] Y. Manassen, R.J. Hamers, J.E. Demuth, and A.J. Castellano, Jr, Phys. Rev. Lett. **62**, 2531 (1988).

[48] I. Hirosawa, K. Akimoto, T. Tatsumi, J. Mizuki, and J. Matsui, J. Crys. Growuth. **103**, 150 (1990).

[49] A. Franciosi, P. Soukiassian, P. Philip, S. Chang, A. Wall, A. Raisanen, and N. Troullier, Phys. Rev. B**35**, 910 (1987);
C.A. Papageorgopoulos, S. Foulias, S. Kennou, and M. Kamaratos, Surf. Sci. **211/212**, 991 (1989).

[50] E. Wimmer, C.L. Fu, and A.J. Freeman, Phys. Rev. Lett. **55**, 2618 (1985).

[51] S. Tsuneyuki, M. Tsukada, H. Aoki, and Y. Matsui, Phys. Rev. Lett. **61**, 869 (1988);
P. Vashishta, R.K. Kalia, J.P. Rino, and I. Ebbsjiö, Phys. Rev. B**41**, 12197 (1990).

[52] R.P. Saxon and B. Liu, J. Chem. Phys. **67**, 5432 (1977);
T.Takada and K.F. Freed, J. Chem. Phys. **80**, 3696 (1983).

[53] R.W. Wyckoff, *Crystal structure*, (Interscience, New York, 1963)

[54] Y. Bar-Yam, S.T. Pantelides, and J.D. Joannopoulos, Phys. Rev. B**39**, 3396 (1989).

Figure captions

Fig. 1-1: Top views of the ideal and reconstructed Si(100) surfaces. The biggest circles are top layer Si atoms, the middle and the smallest circles are second and third layer Si atoms, respectively.

Fig. 2-1: The total energies of the silicon crystal with changing lattice constant according to the present calculation with use of the gaussian basis set. The exponents of the gaussian are shown in section 2.2.

Fig. 2-2: The unit cell and atomic configuration of the α–quartz.[53] Open and dotted circles mean the Si and O atoms, respectively. The upper one is the projection from the 'c' axis and the lower one is the side view. The boundary of the unit cell is shown as the dot–dash lines. The atoms drown by solid lines are located in the unit cell. The others drown by dotted lines are located in the neighboring unit cells.

Fig. 2-3: The total energies of the α–quartz with changing lattice constant of the 'a' axis according to the present calculation with use of the gaussian basis set. The exponents of the gaussian are shown in section 2.2.

Fig. 3-1: The projection of the unit cell of the slab of the Si(100)2×1 surface from the (011) crystallographic axis. The axis of the C_2 symmetry is marked at the center of the unit cell. There are two equivalent surfaces on both sides of the slab.

Fig. 3-2: The top view of the 2×1 and 2×2 unit cells on the Si(100) surface. The two Brillouin zones are exhibited just below the corresponding unit cells. The dots mean the k-points which are used for the momentum space integration for the band calculations.

Fig. 3-3: The four target areas of adsorbed O_2 molecule. The site A is just on the dimer, B is between the neighboring dimers. The sites C and D are between the neighboring two dimers rows.

Fig. 3-4: Dissociation of the O_2 molecule on the site A. Open and dotted circle mean the Si and O atoms, respectively. The two arrows indicate the calculated forces on each O atom: 0.137Ry/a.u. in the upper O atom, and 0.085Ry/a.u. in the lower. The contour map is the valence charge density on the (011) plane. The highest value of the contour line is 1.4electron/(a.u.)^3. The sequent contour lines differ by a factor of 2.

Fig. 3-5: The sequence of the geometry optimization of the O_2 molecule on the site B. The projections from the (011) axis are shown in the left hand side and those of the $(01\bar{1})$ axis are shown in right hand side. The arrows indicate the calculated forces. The final stable structure is shown in the bottom.

Fig. 3-6: Dissociation of the O_2 molecule on the site B. The projection is from the same direction as those of the right hand side in Fig. 3-5. The highest contour line is 1.1electron/(a.u.)^3. The sequent contour lines differ by a factor of 2.

Fig. 3-7: The sequence of the geometry optimization of the O_2 molecule on the site C shown from the two directions as same as those in Fig. 3-5.

Fig. 3-8: Schematic diagram of the electronic configurations of the O_2 molecule before and after the electron transfer from the Si(100) surface. The components of the O $2s$ orbitals are not shown here.

Fig. 3-9: The metastable configuration of the adsorbed O atom. The Si dimer and the O atom are located on the (011) plane. The top view in the upper panel exhibits the stability of the O atom against the displacement away from the plane.

Fig. 3-10: The most stable geometry of the adsorbed O atom which intervenes the dimer. The charge contour map in the (011) plane is shown in Fig. 3-10(b) in which the maximum value of the contour lines is 1.1electron/(a.u.)^3. The sequent contour lines differ by a factor of 2. The Si–O–Si bond shows an ionic feature.

Fig. 3-11: Top and side views of the metastable O atom on the Si(100) surface. The O atom is located apart from the (011) plane and the surface Si dimer is twisted and buckled.

Fig. 3-12: Schematic diagram of the symmetric stretching mode of the Si–O–Si complex on the Si(100) surface. The directions of the vibration of Si and O atoms are denoted by the arrows. However the ratio of the lengths of the arrows does not correspond to the exact ratio of the atomic displacements of the Si and O atoms.

Fig. 3-13: The UPS spectrum of the oxygen adsorbed Si(100) surface at several oxygen coverage by Hollinger et al.[18] The L (Langmuir) means the unit of the oxygen exposure which corresponds to 1×10^{-6}Torr $\cdot$ sec. The arrows denote the positions of the surface states. The typical three peaks marked B, C^1, and C^2 appear after the sample annealing at $700°C$ after 1000L oxygen exposure, i.e. 1.5ML oxyen coverage.

Fig. 3-14: The calculated DOS with the corresponding geometries. The dotted line means the Fermi level. The O $2s$ level is too deep to compare the experimental results.[18] The three arrows denote the typical peaks in the valence band region upon oxidation.

Fig. 3-15: The calculated LDOS of the surface Si and O atoms corresponding to the geometry of Fig. 3-10 and the DOS of Fig. 3-14(c). The highest peak of the three denoted in Fig. 3-14(c) can be assigned to the LDOS of the O p_x and p_z orbitals and the lowest peak can be assigned to the O p_y orbital.

Fig. 3-16: The top and side views of the 1ML O atoms on the Si(100) surface. The O atoms are located $0.11\mathring{A}$ above the surface Si atoms.

Fig. 3-17: The side view and charge contour map of the adsorbed O atoms on the 1ML oxygen covered surface. The atoms drown by the solid lines are located in the $(01\bar{1})$ plane. The others drown by the dotted line are located apart from the plane. The maximum value of the contour lines is 1.1electrons/(a.u.)^3. The sequent contour lines differ by a factor of

2. The charge density show us the ionic feature of the Si–O bonds of the newly adsorbed O atoms.

Fig. 3-18: The top and side views of the stable structure of the 3ML oxidized Si(100) surface. The surface O and Si atoms are lifted up. The same sequential numbers are assigned to the equivalent atoms. The local atomic configuration is similar to that of the stishovite.

Fig. 1-1

(a)

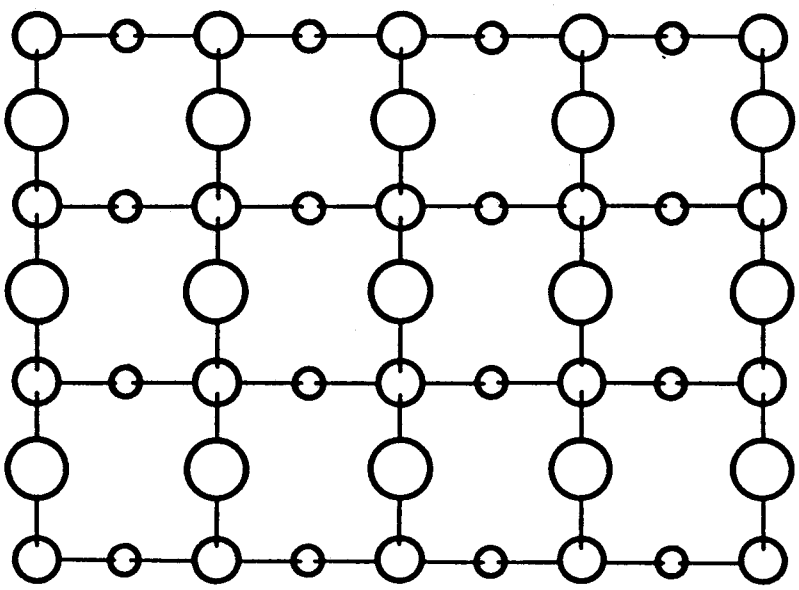

Ideal

(b)

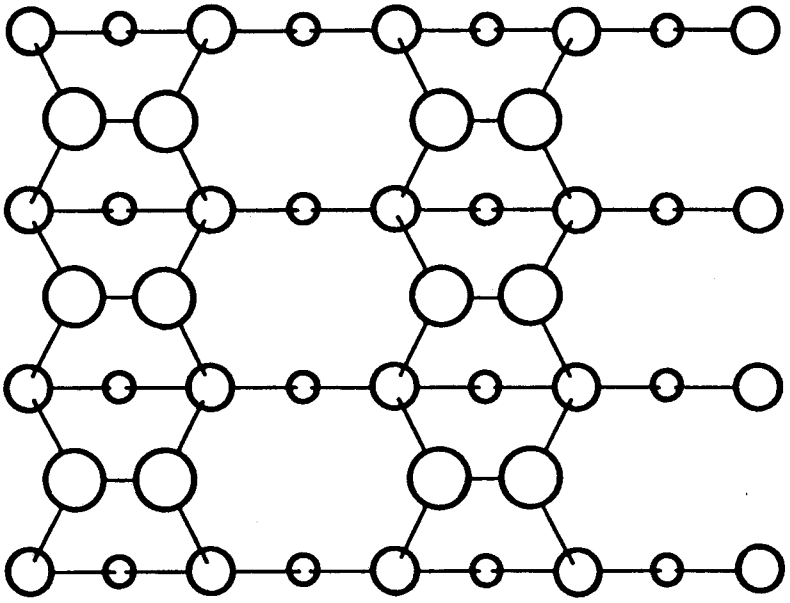

Relaxed

Fig. 2-1

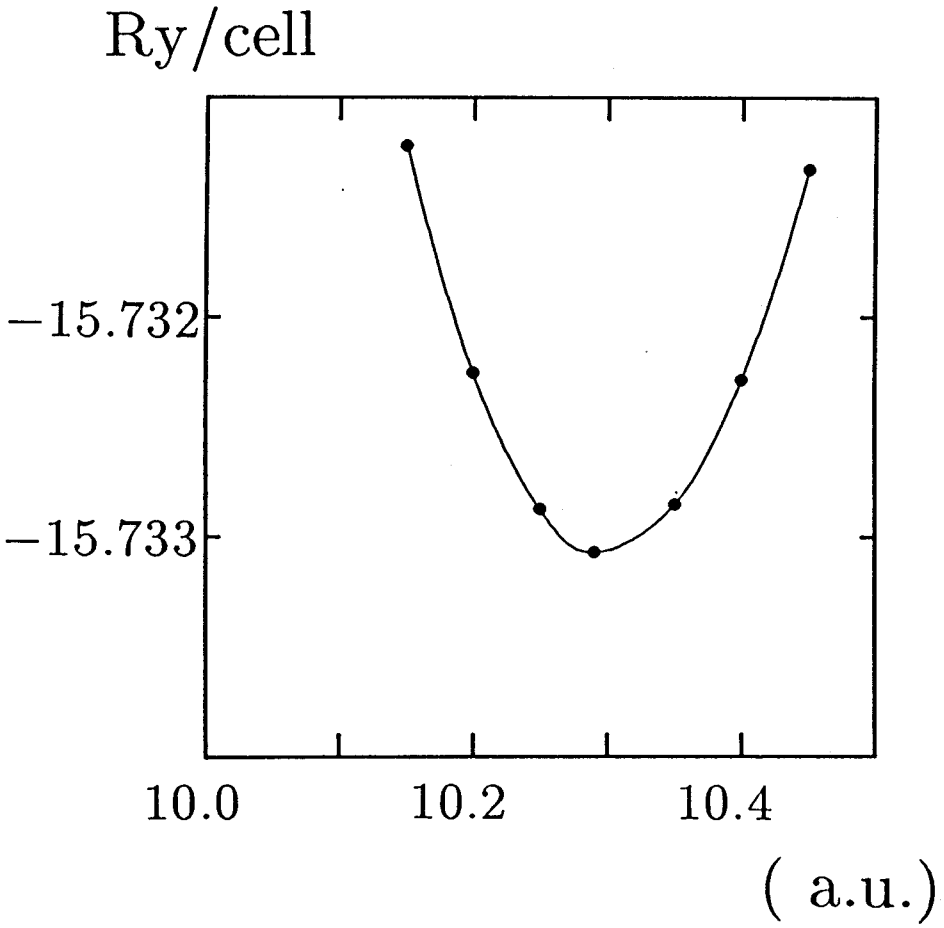

Fig. 2-2

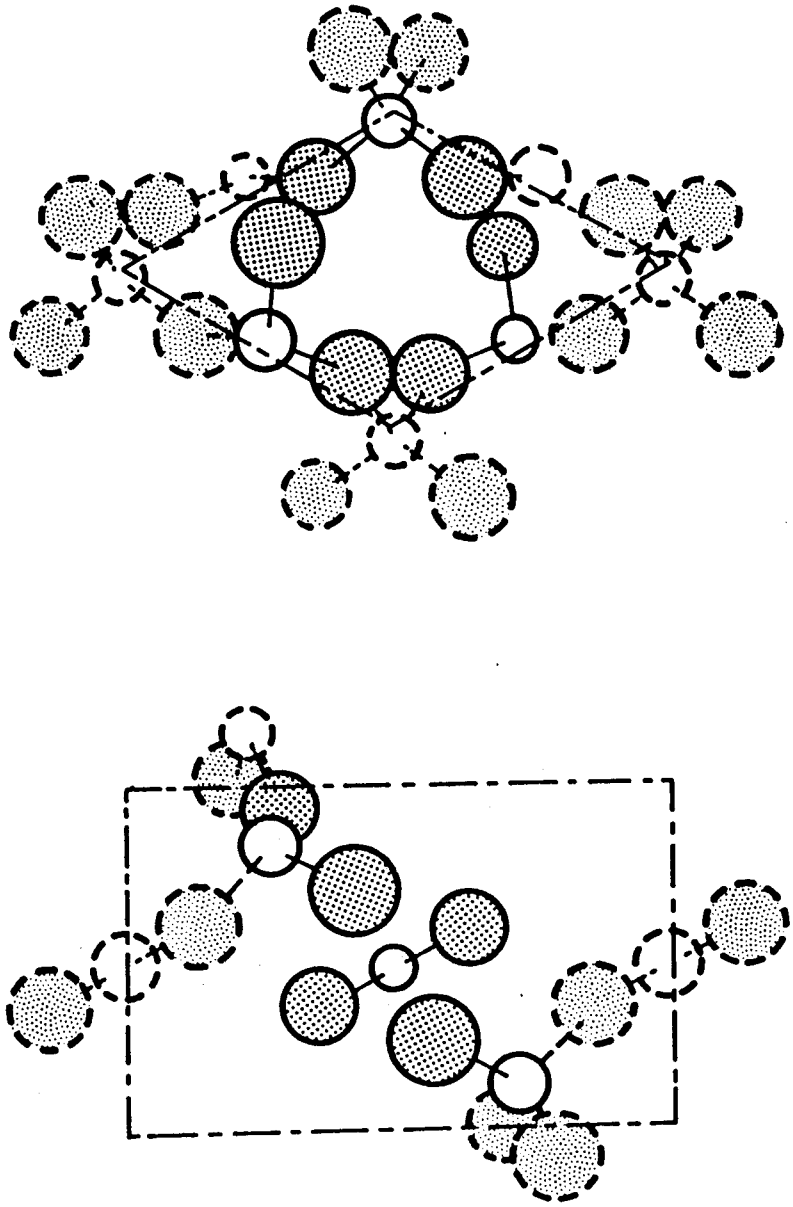

Fig. 2-3

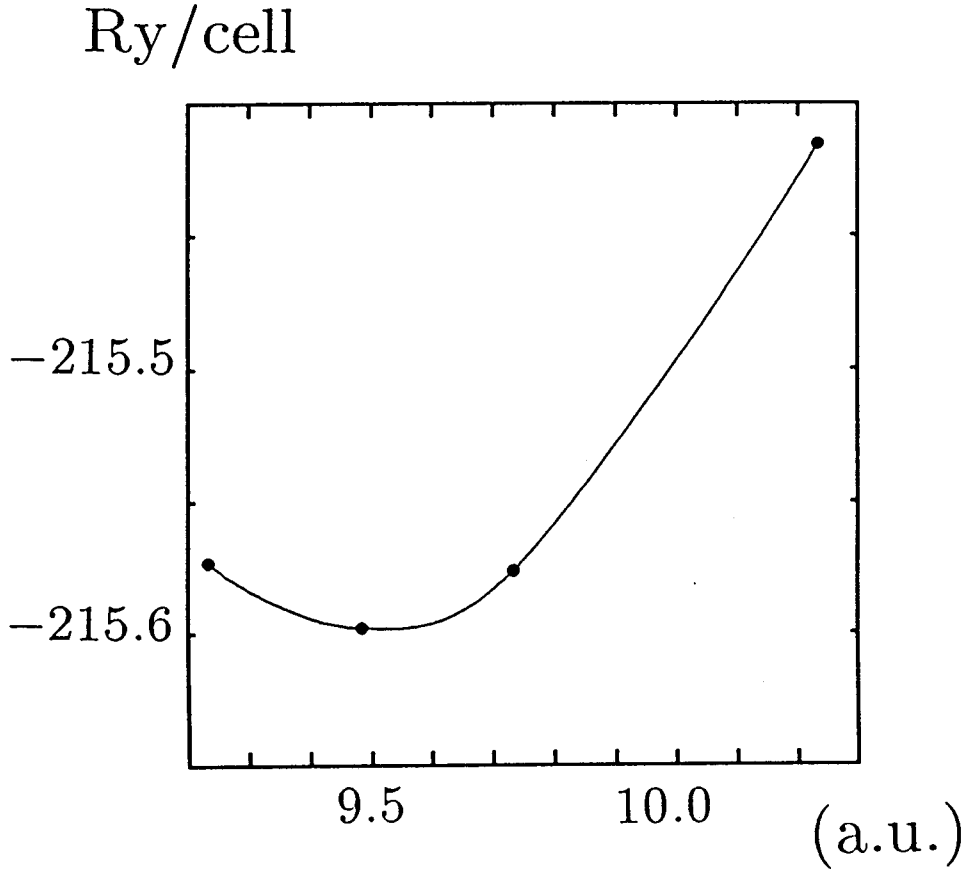

Fig. 3-1

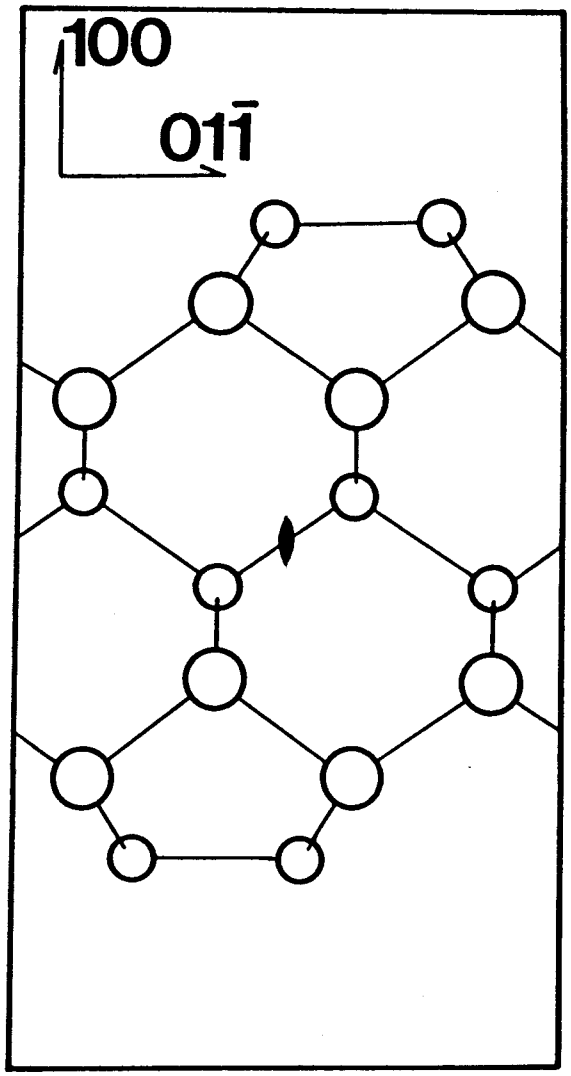

Fig. 3-2

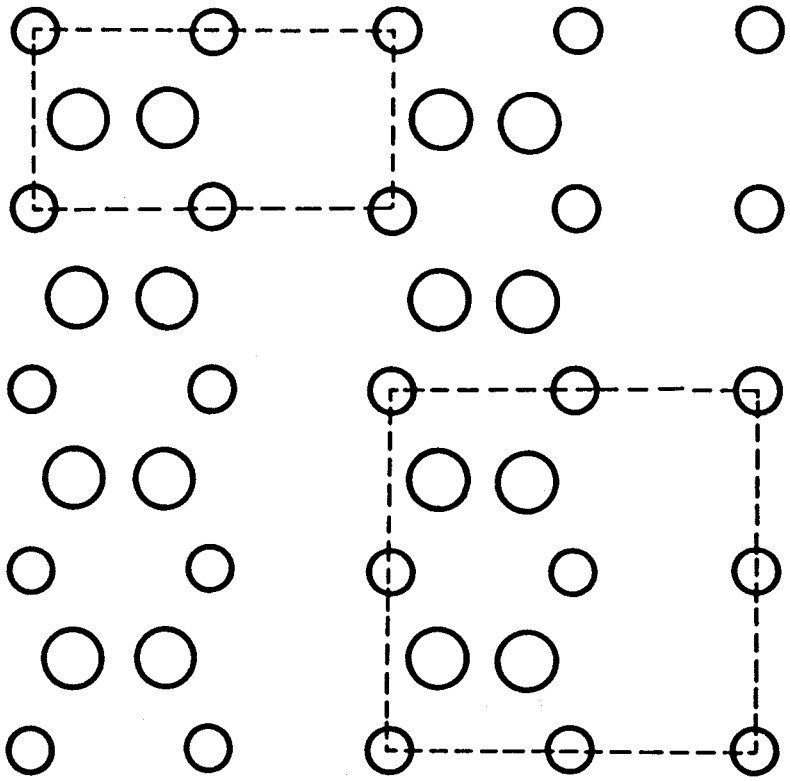

Unit cells

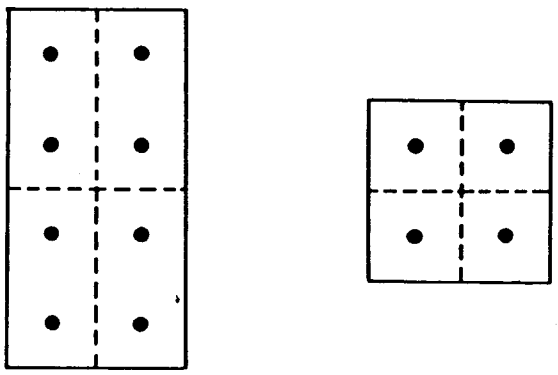

The first Brillouin zones

Fig. 3-3

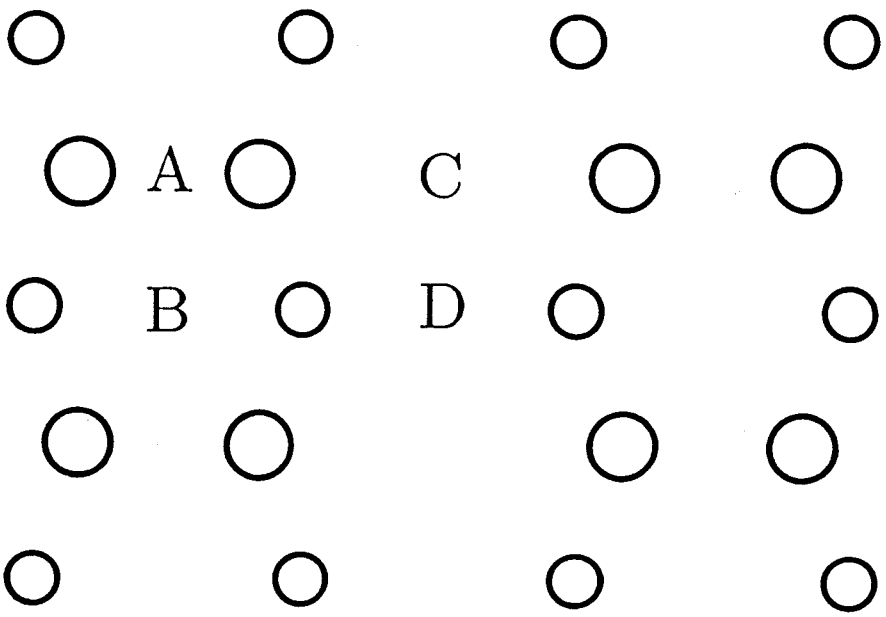

Fig. 3-4

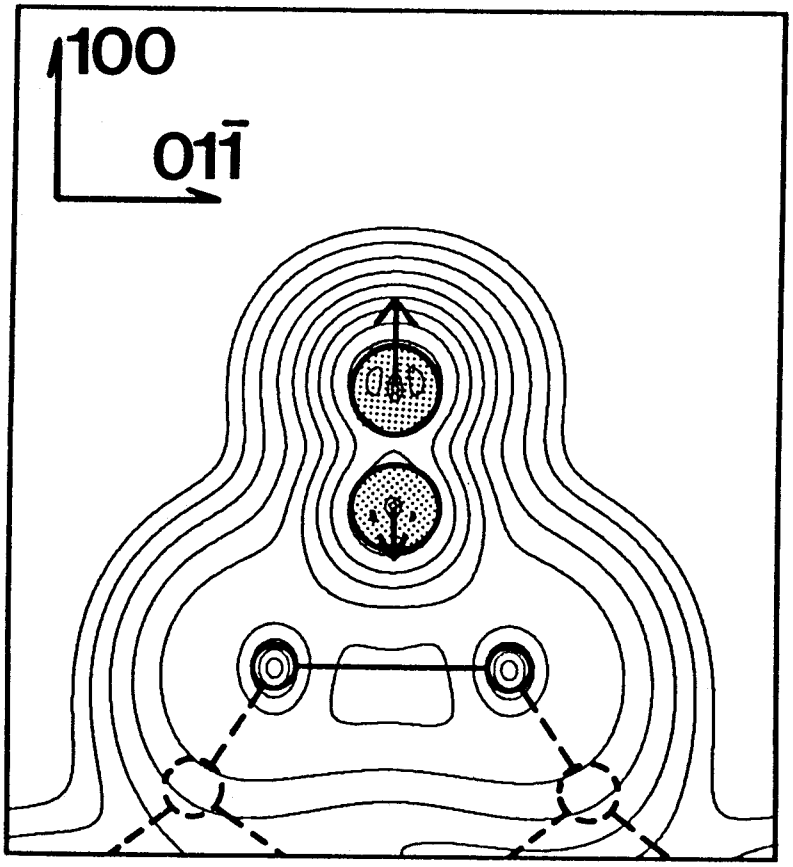

Fig. 3-5

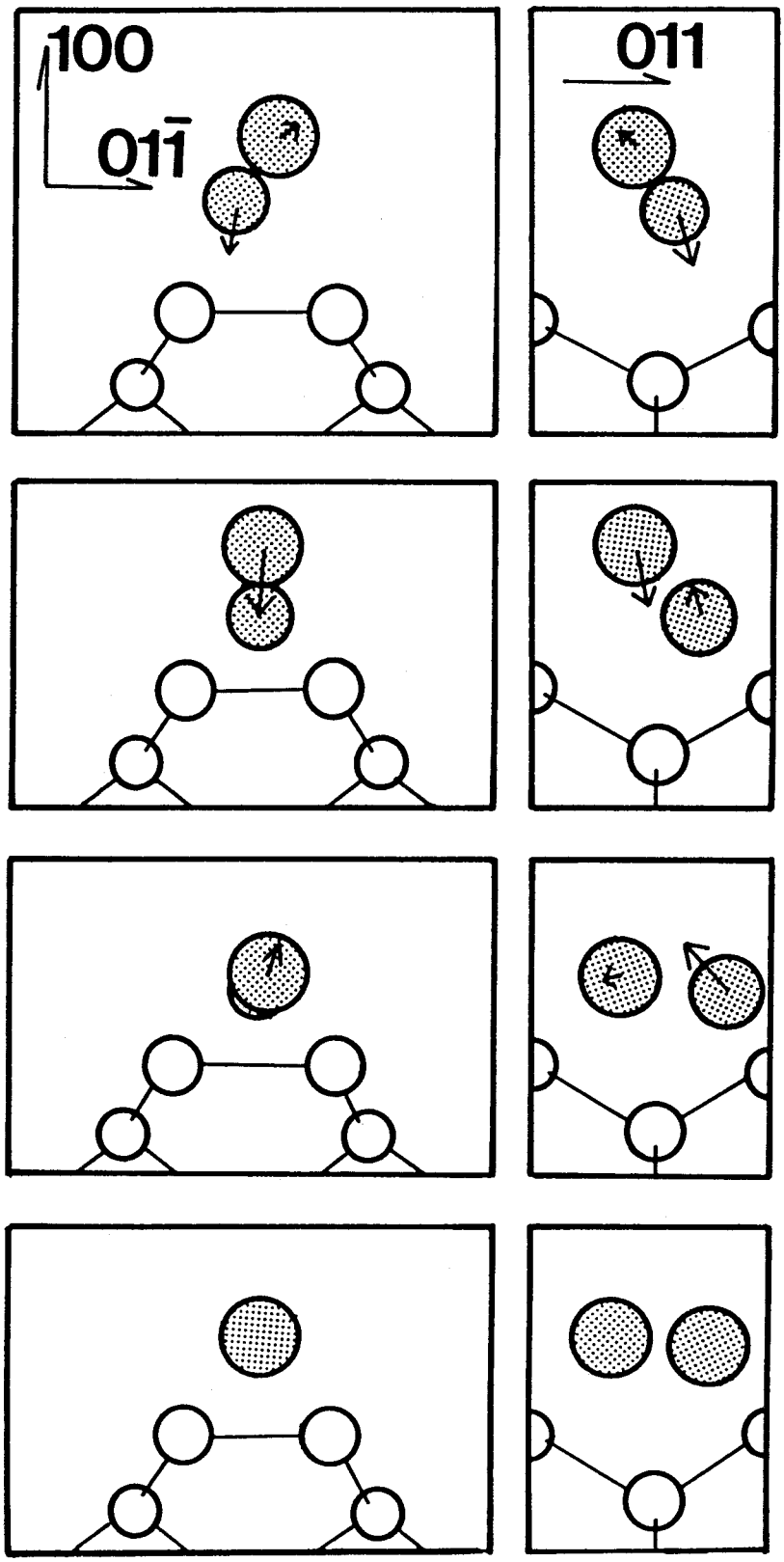

Fig. 3-6

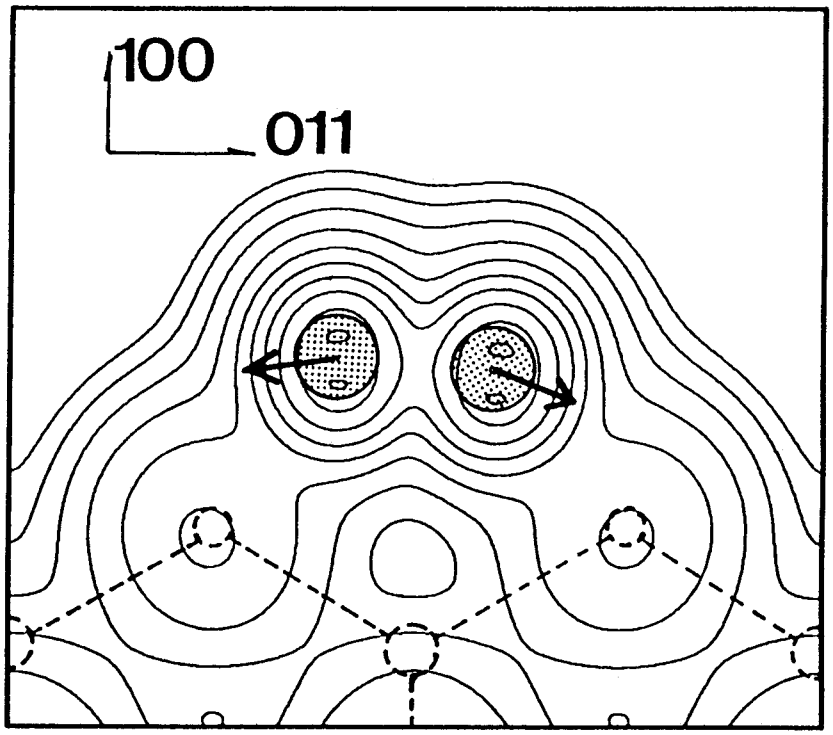

Fig. 3-7

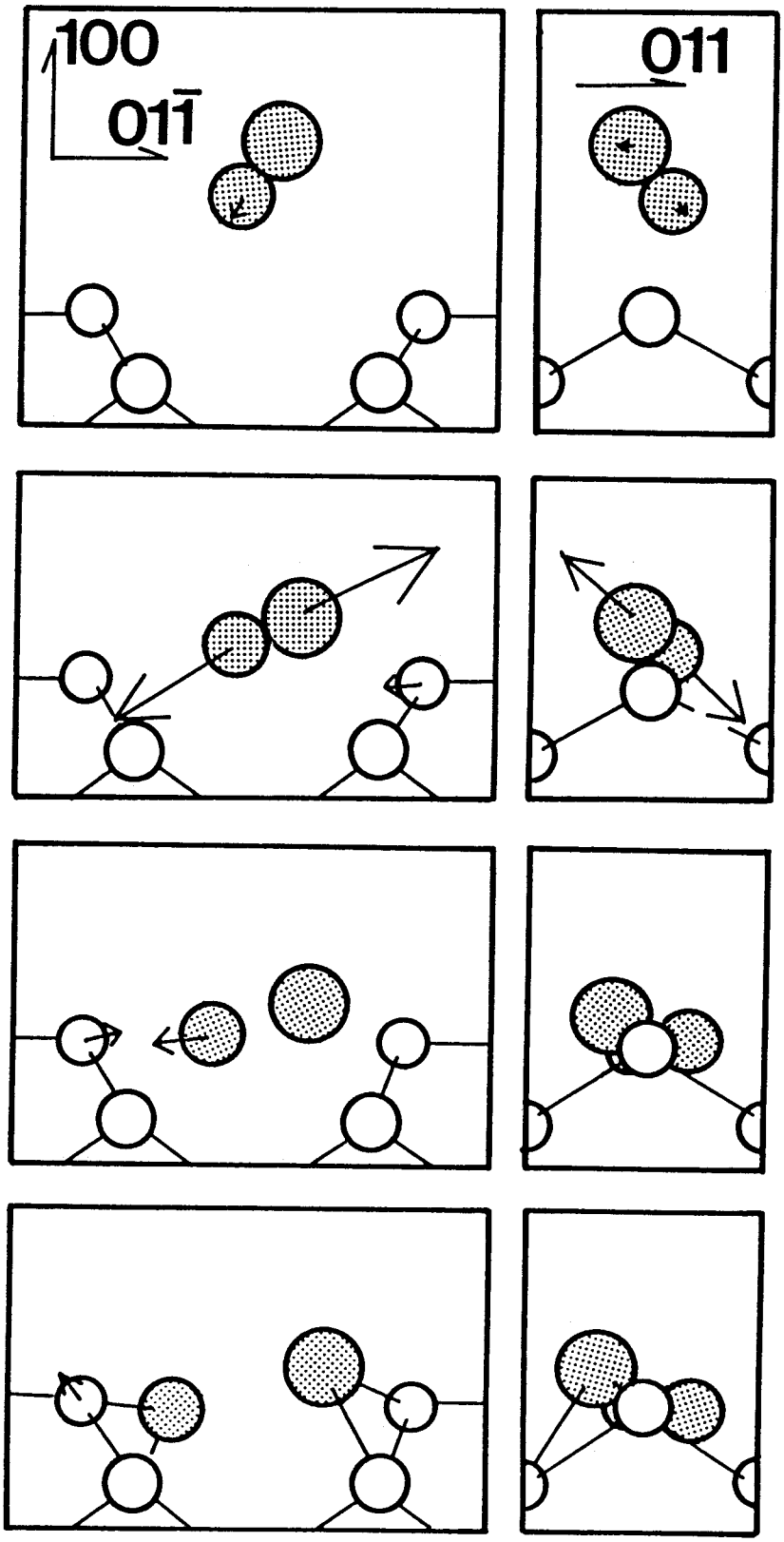

Fig. 3-8

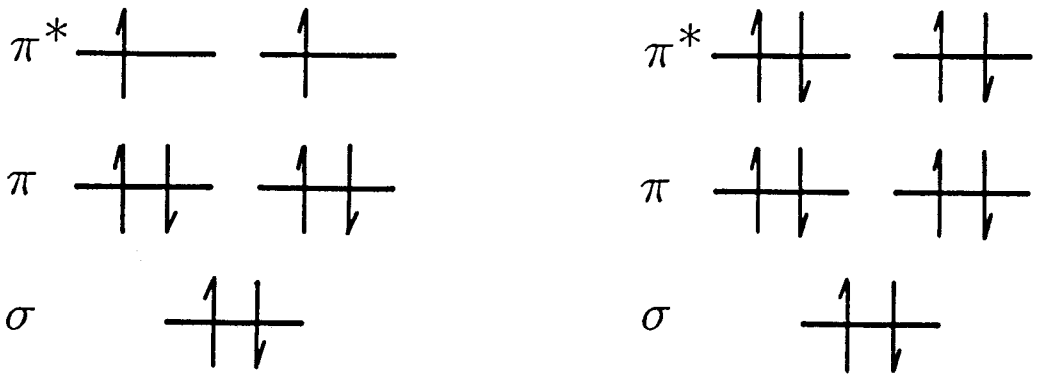

Fig. 3-9

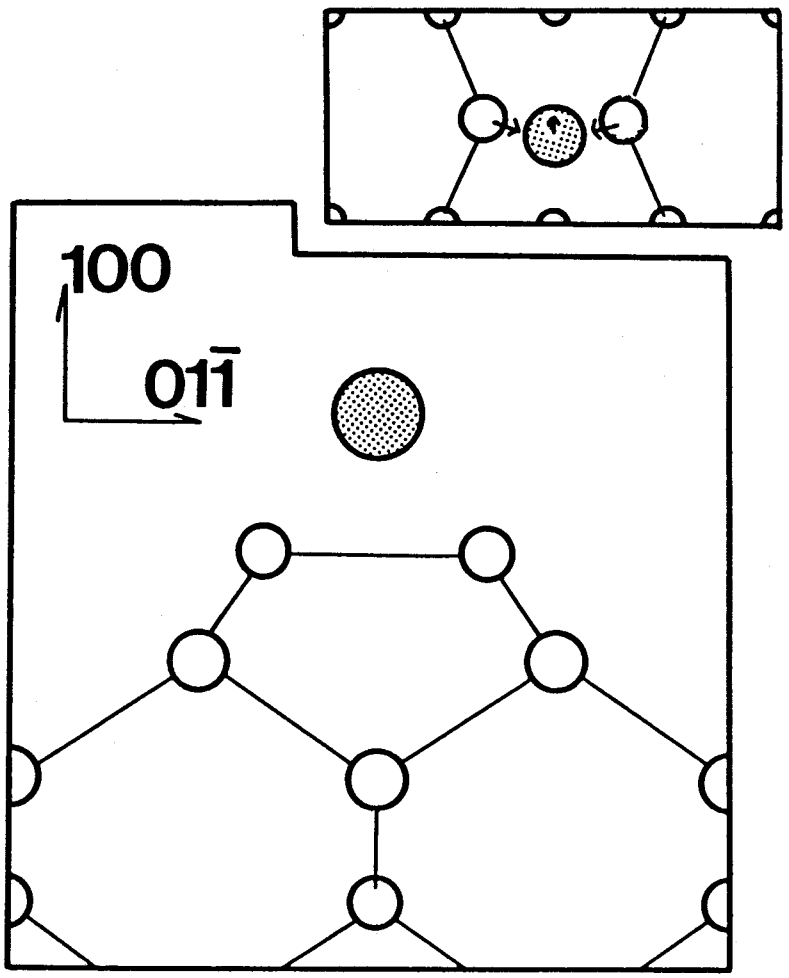

Fig. 3-10(a)

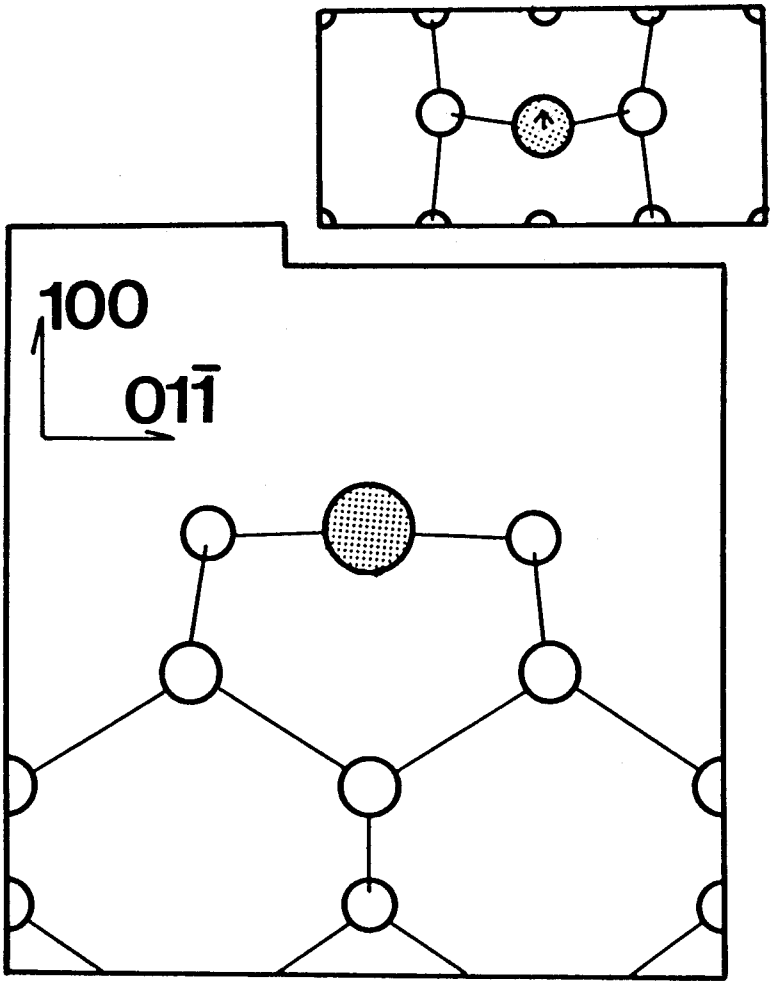

Fig. 3-10(b)

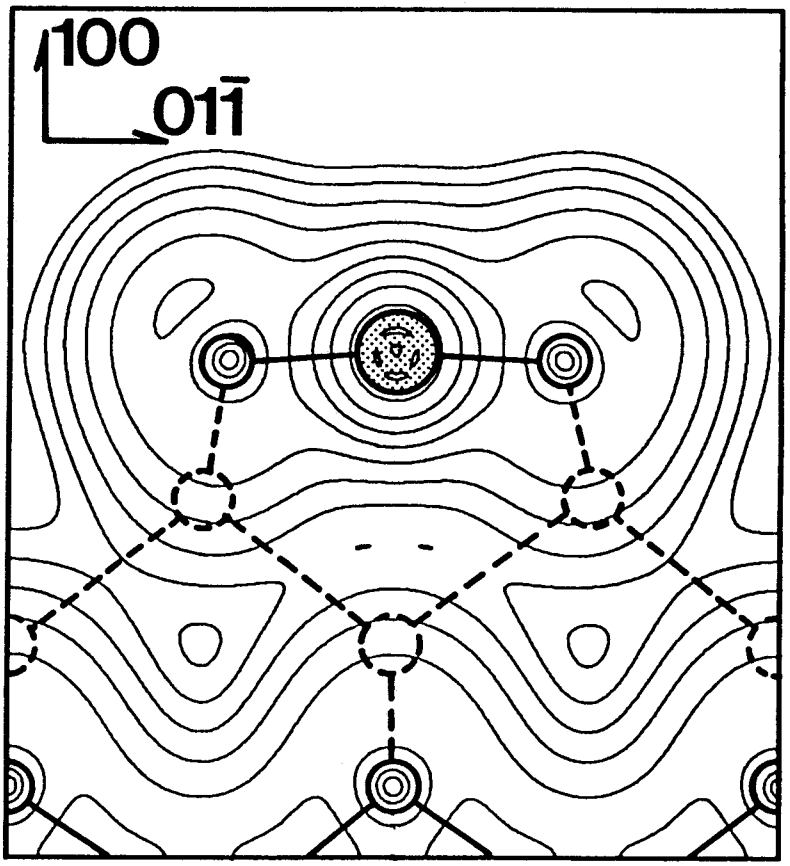

Fig. 3-11

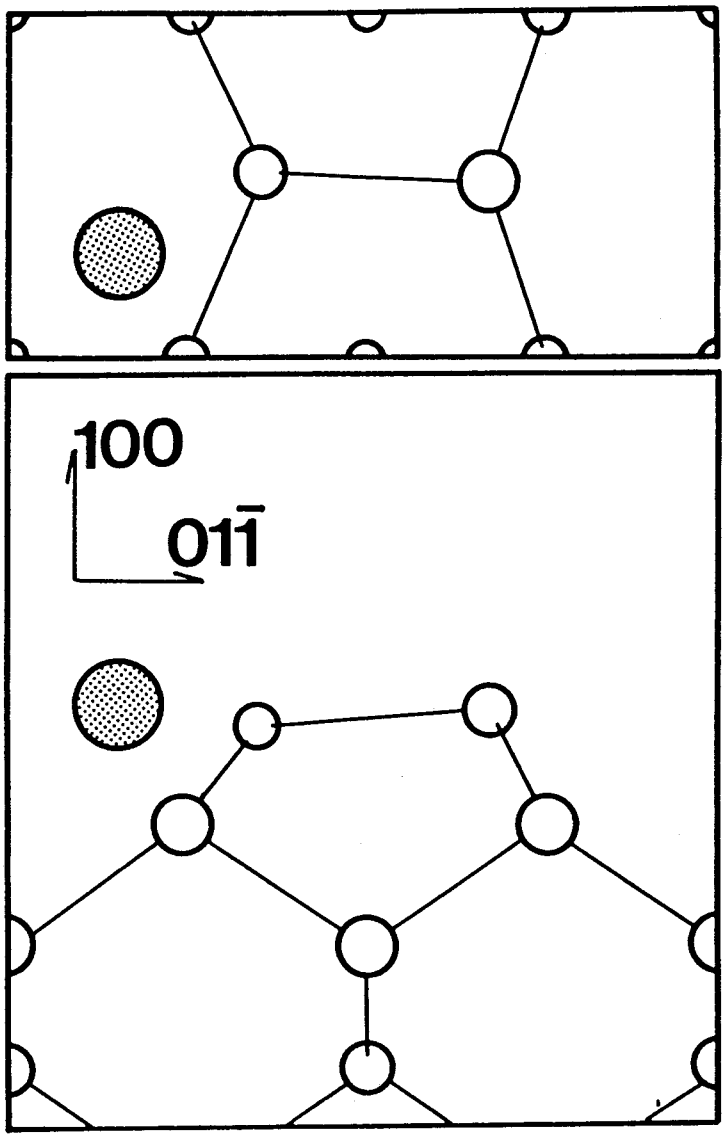

Fig. 3-12

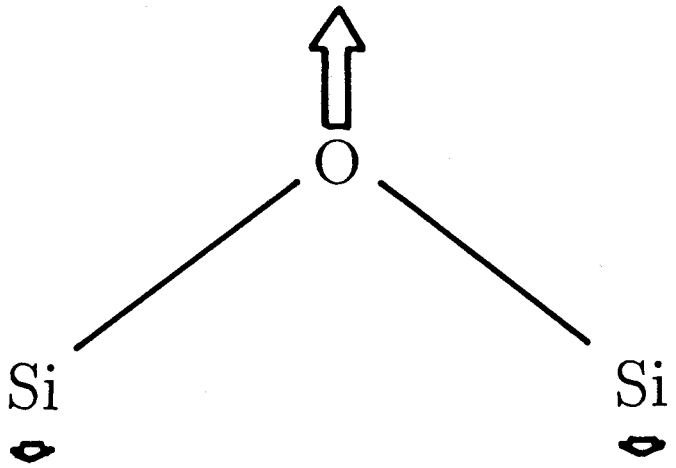

Fig. 3-13

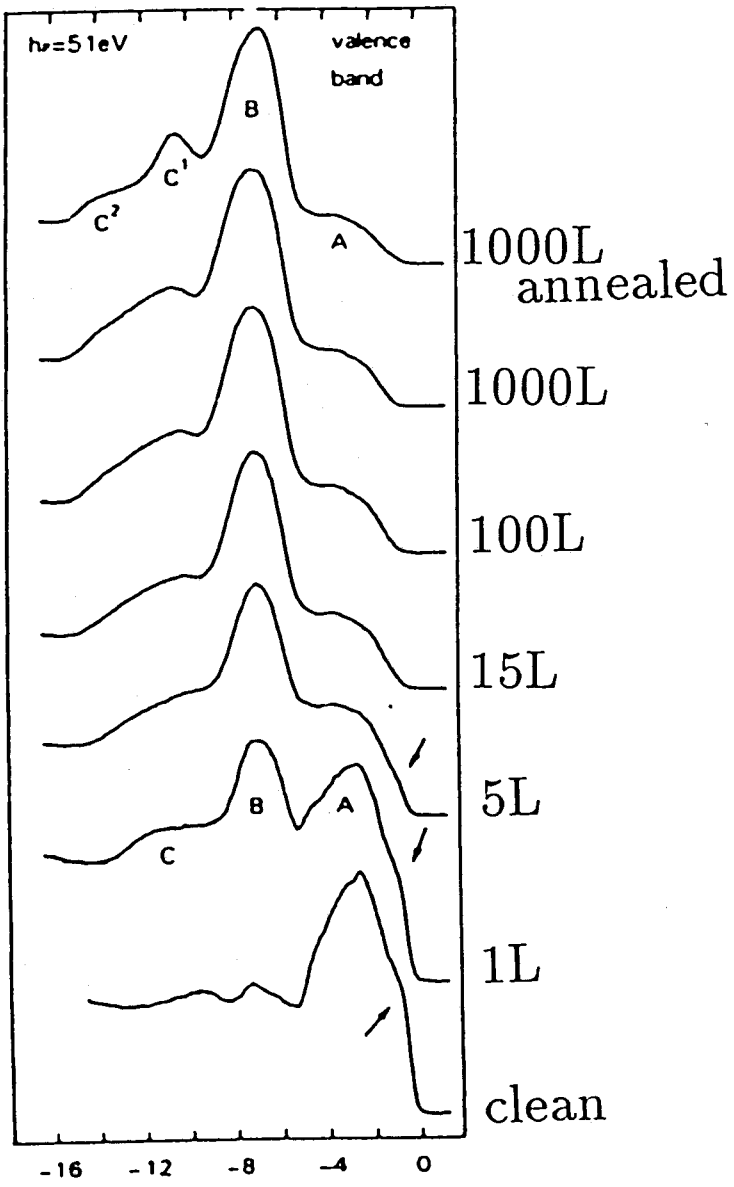
hν=51eV
valence
band
B
C'
C²
A
1000L
annealed
1000L
100L
15L
B
A
C
5L
1L
clean
-16
-12
-8
-4
0
initial energy (eV)

Fig. 3-14

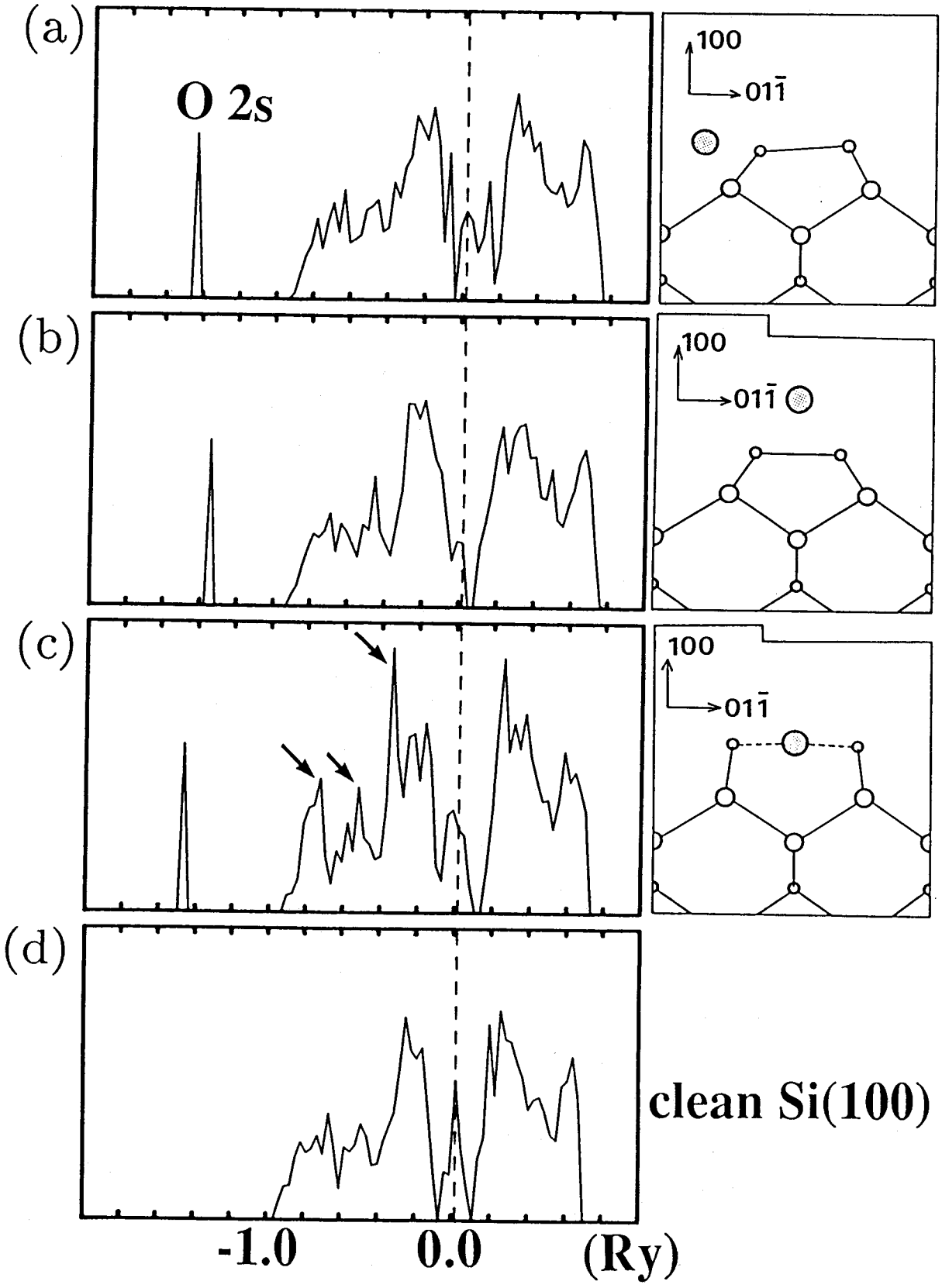
(a)
O 2s
100
01$\bar{1}$
(b)
100
01$\bar{1}$
(c)
100
01$\bar{1}$
(d)
clean Si(100)
-1.0
0.0
(Ry)

Fig. 3-15

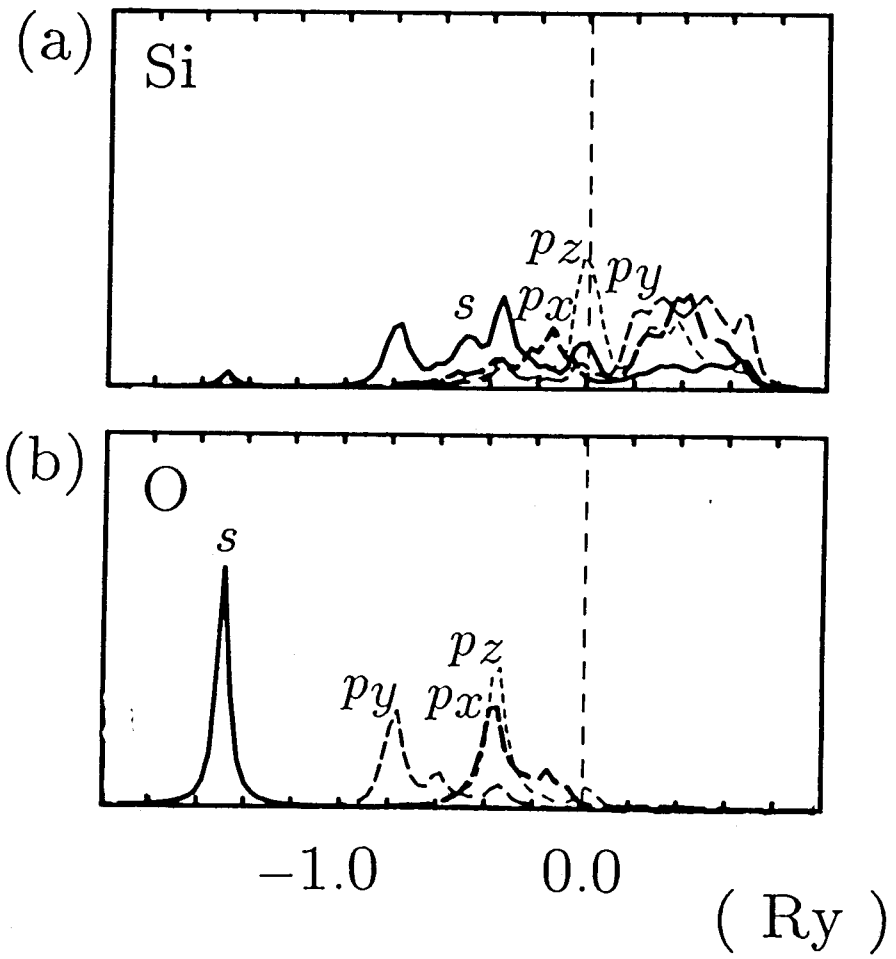

Fig. 3-16

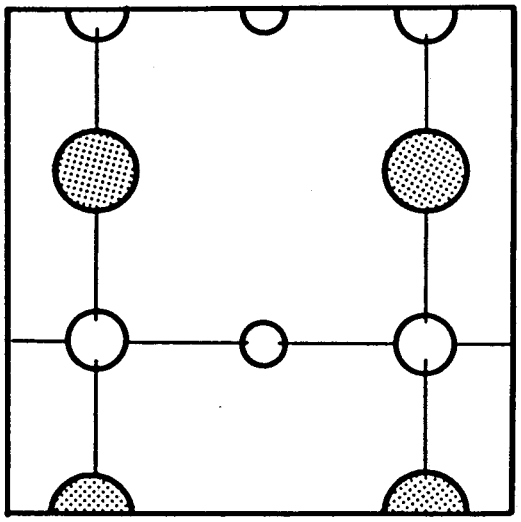

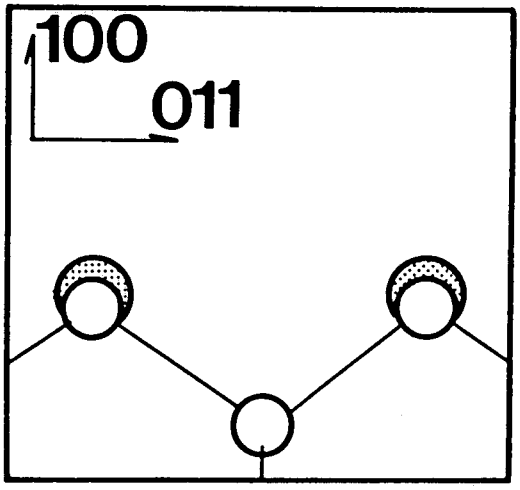

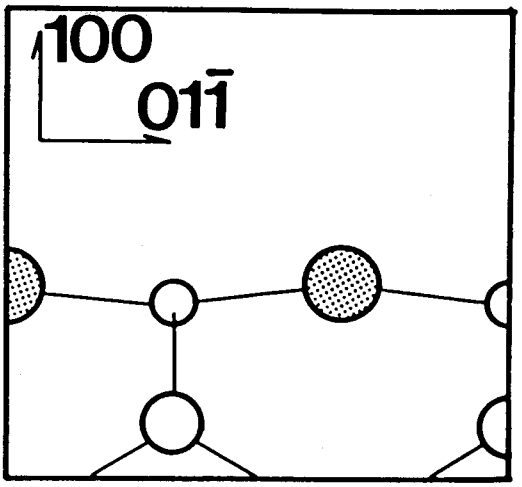

Fig. 3-17

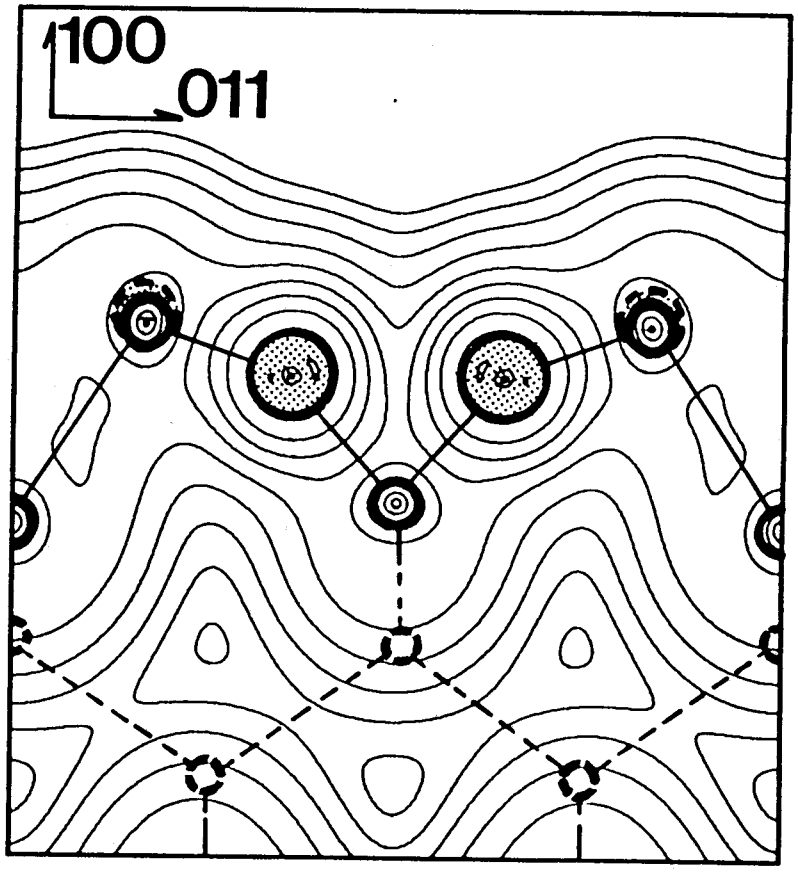

Fig. 3-18